

Hazards Induced by Breach of Liquid Rocket Fuel Tanks: Physics-Based Modeling of Cavitation- Induced Self-Ignition and Radiation-Induced Aerosol Explosion of Cryogenic H₂-O₂ Fluids



Ekaterina Ponizovskaya-Devine
Viatcheslav Osipov
Cyrill Muratov
Halyna Hafiychuk
Vadim Smelyanskiy

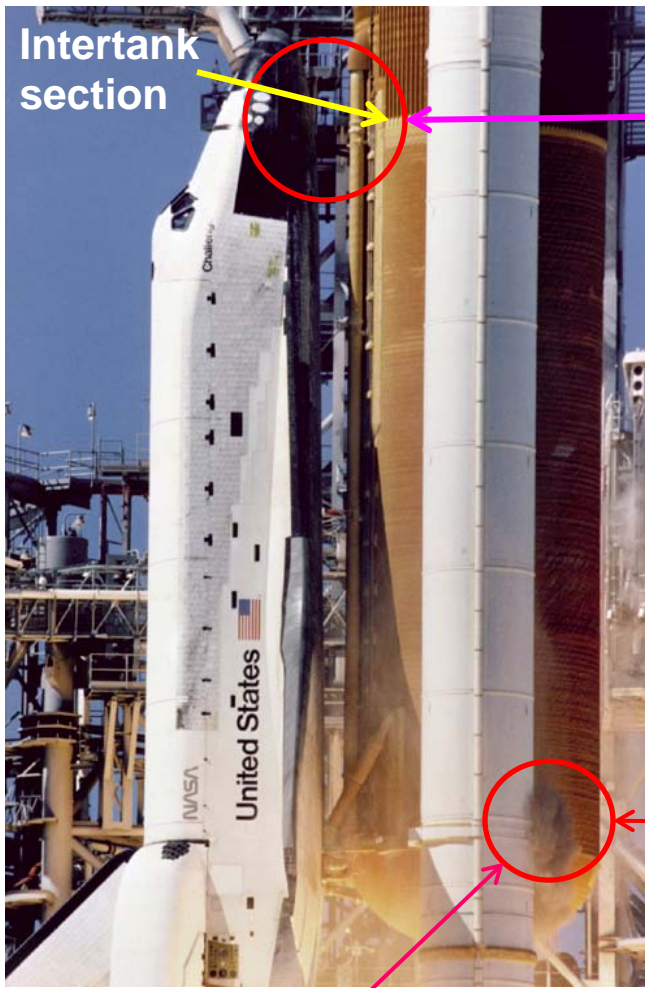
Physics Based Methods, Ames - NASA



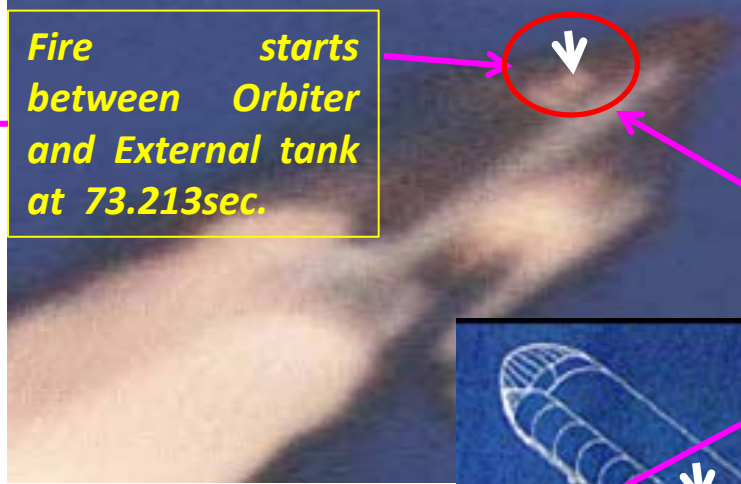
The Challenger disaster.
Problem: fire starts at intertank section



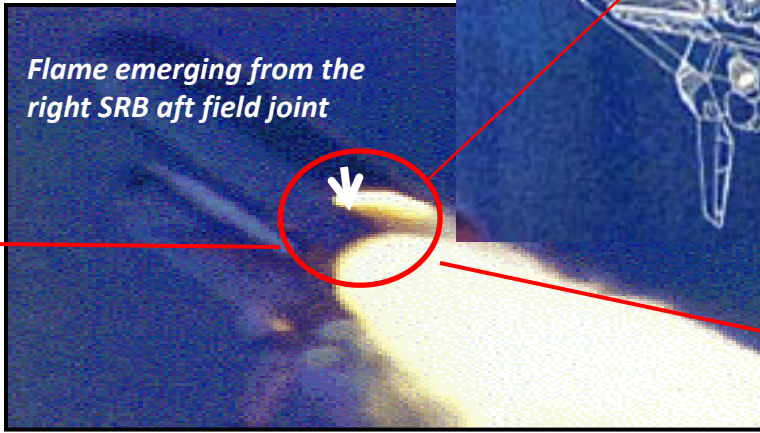
Before start



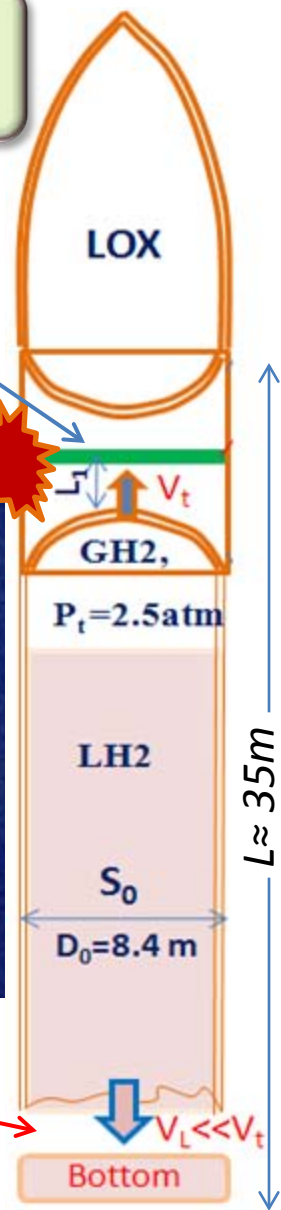
Fire starts between Orbiter and External tank at 73.213sec.



Intertank section



Flame emerging from the right SRB aft field joint



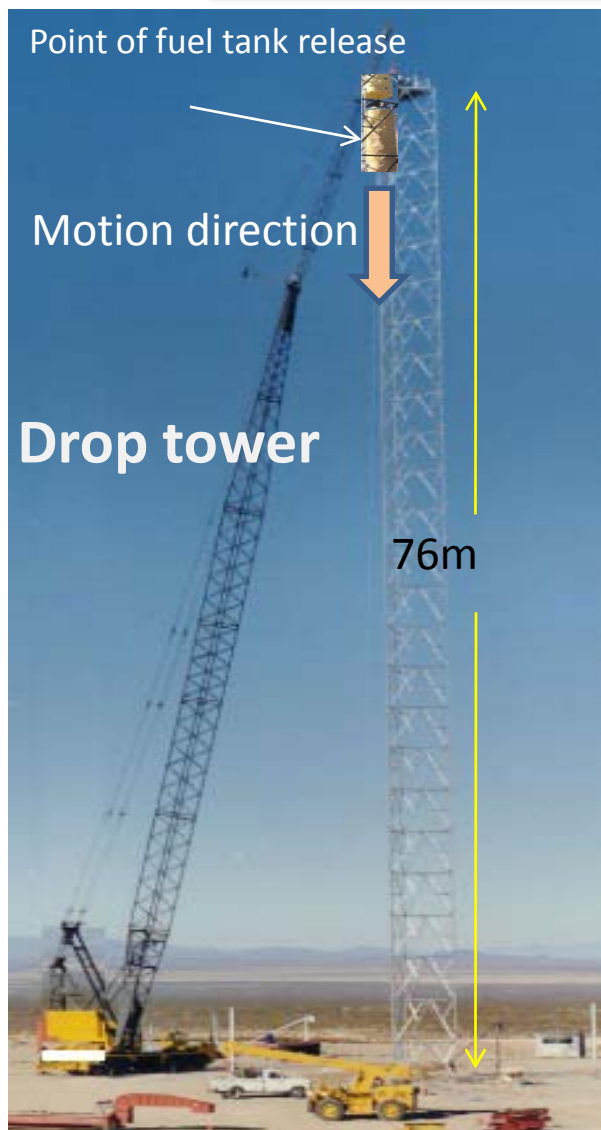
Dark smoke from SRB leak appears on the ground beginning 0.678 sec after ignition of the boosters

Source of ignition near the broken interface, localized far from hot nozzle gas was puzzling

Cole, M.D., "Challenger: America's space tragedy", Springfield, N.J., Enslow Publishers, 1995.
•Report of the Presidential Commission on the Space Shuttle Challenger Accident, DIANE Publishing, 1986, 256 pages

1. Review of the hydrogen-oxygen vertical impact (HOVI) tests.
2. Detailed analysis of detonation and deflagration flames in GH₂/GO_x/air mixtures.
3. Key differences between the HOVI test data and the conventional deflagration and detonation.
4. The proposed mechanism of the explosion of GH₂/GO_x mixture .
5. Analysis of experimental data of HOVI tests: Energy and velocity of shock waves.
6. Estimation of effective H₂ and O₂ masses.
7. Dynamics of escape of H₂ and O_x liquids from ruptured tanks.
8. Evaporation of escaped cryogenic LH₂/LO_x on hot ground.
9. Fragmentation of escaped liquid streams and formation of droplets (aerosols) as a result of vertical impact of the ruptured tanks. Structure of sprays.
10. Conductive and radiative evaporation of LH₂ droplets.
11. Flame acceleration by aerosol combustion.
12. Interpretation of HOVI 9 and other tests.
13. Cavitation-induced scenarios of ignition of GH₂/GO_x/LO_x cryogenic mixtures and formation of their detonation or deflagration.

Hazards induced by breach of liquid fuel tanks (H_2/O_2 vertical impact (HOVI) tests)



11/16/2012

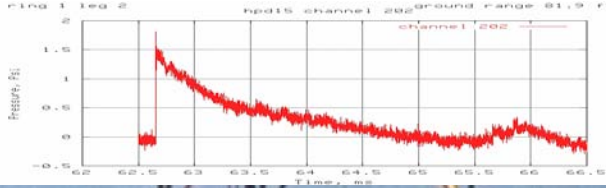
Hydrogen/Oxygen Vertical Impact (HOVI) tests

LOx and LH₂ tanks in HOVI 9, 13, and 14 were fixed on a 76 m (250 ft)-high drop tower. Then both tanks were dropped to the ground. In HOVI 2 and 5 only LOx tank was dropped to the LH₂ tank situated on the ground .

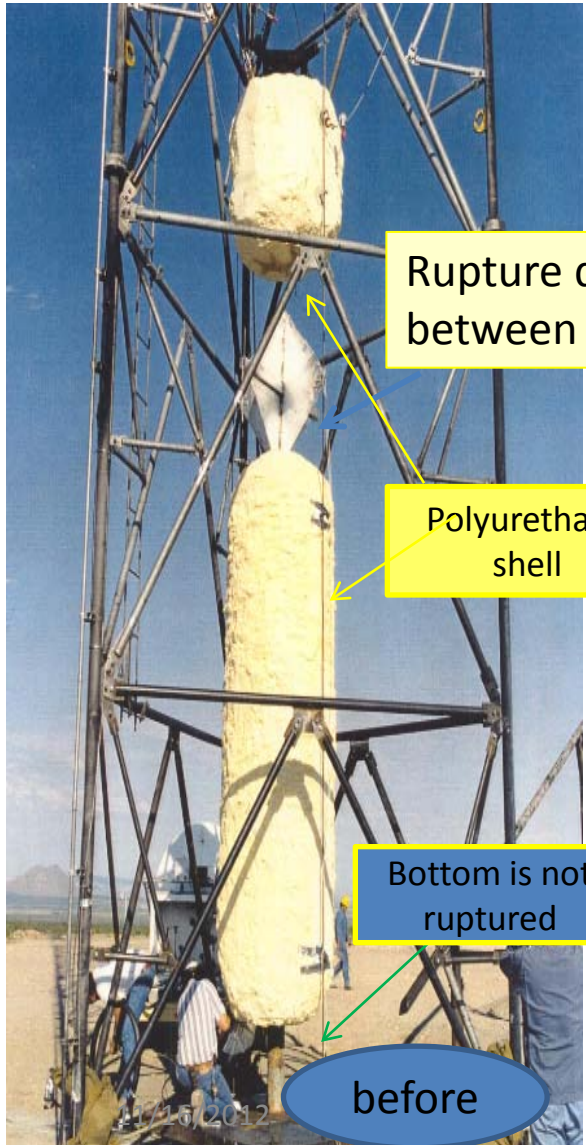
The impact velocity was within 30÷35m/sec.

The main purpose of these tests was to obtain explosion data that would be more typical or more representative of a launch vehicle failure than the distributive mixture tests.

Group 1 (Test 15)



Yield from 0.5 to 3.2 percent.
Cloud briefly visible before ignition. Prompt ignition.

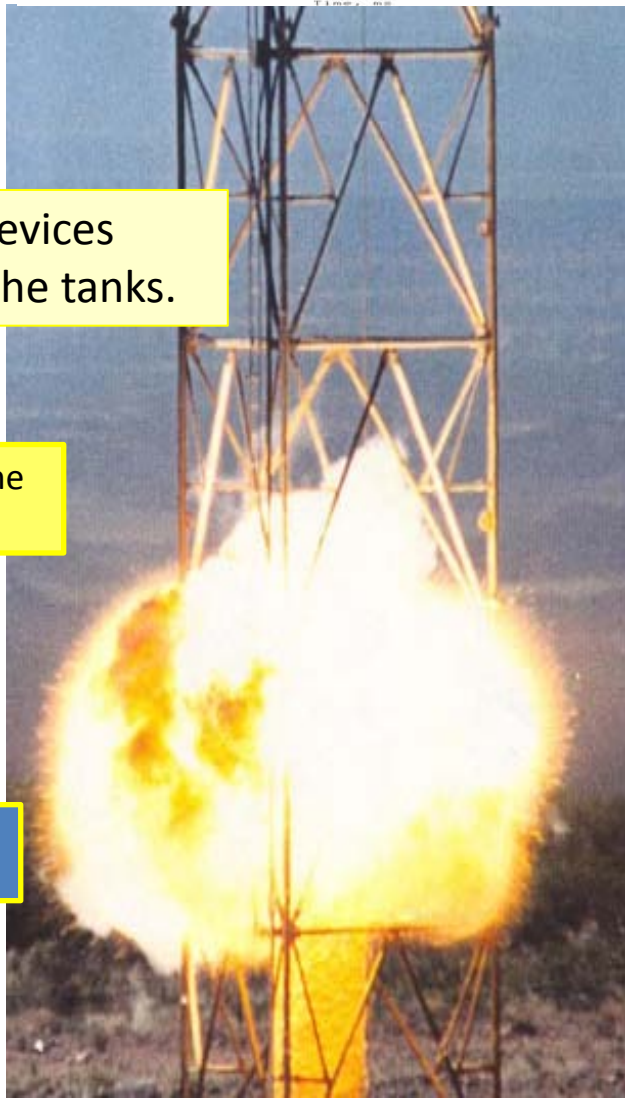


Rupture devices between the tanks.

Polyurethane shell

Bottom is not ruptured

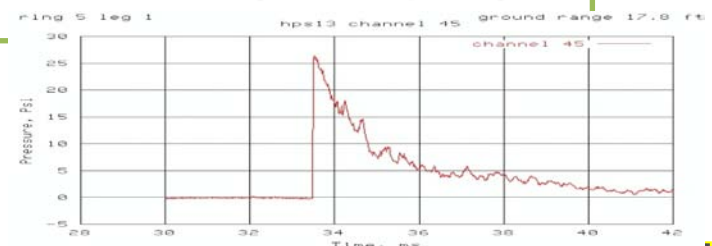
before



after

Group 2: Yield is below about 2 percent.
Prompt ignition.

Test 13.



- Analysis of detonation and deflagration as stable modes of combustion is based on published work and our simulations
- Study of detonation characteristics as functions of H₂/O₂/N₂ mixture composition and conditions necessary for detonation initiation
- Analysis of the main parameters of turbulent deflagration flames in premixed H₂/O₂/N₂ mixtures
-
- Comparison of detonation and deflagration combustion characteristics with HOVI data

$$k_f = A T^b \exp(-E/RT)$$

output data:

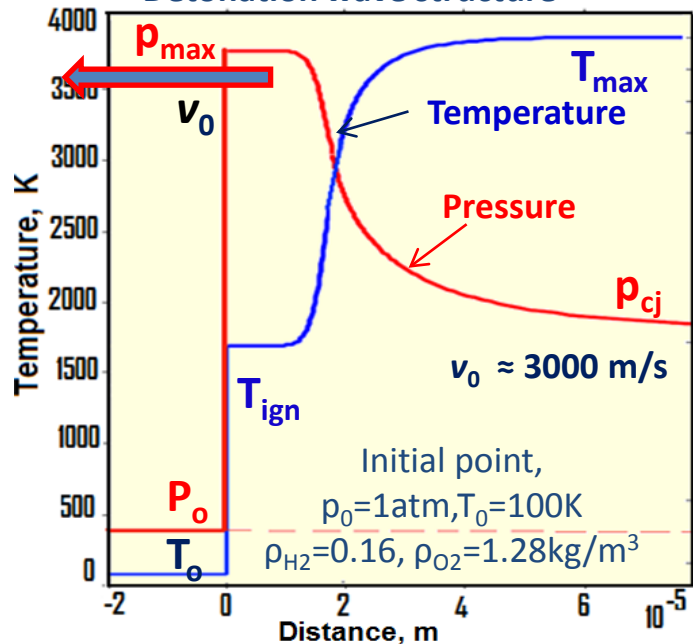
Reaction	A	b	E (cal/mol)
Hydrogen-oxygen mechanism (CANTERA)			
$H_2 + O_2 = OH + OH$	1.70×10^{13}	0	47 780
$H_2 + O_2 = H O_2 + H$	2.57×10^{12}	0	19626
$H + O_2 = OH + O$	2.65×10^{16}	-0.67	17 041
$O + H_2 = OH + H$	5.06×10^4	2.67	6290
$OH + H_2 = H_2O + H$	1.17×10^9	1.3	3626
$OH + OH = H_2O + O$	6.30×10^8	1.3	0
$H + OH + M = H_2O + M$	1.60×10^{22}	-2.00	0
$H + H + M = H_2 + M$	1.00×10^{18}	-1.00	0
$H + O + M = OH + M$	6.00×10^{16}	-0.6	0
$H + O_2 + M = H O_2 + M$	3.61×10^{17}	-0.72	0
$H O_2 + H = H_2 + O_2$	1.25×10^{13}	0	0
$H O_2 + H = OH + OH$	1.40×10^{14}	0	1073
$H O_2 + H O_2 = H_2 O_2 + O$	2.00×10^{12}	0	0
$H O_2 + O = O_2 + OH$	1.40×10^{13}	0	1073
$H_2 O_2 + OH = H_2 O + H O_2$	1.00×10^{13}	0	1800
$O + OH = H + O_2$	3.61×10^{14}	-0.5	0
$H + H_2 O_2 = H_2 + H O_2$	1.6×10^{12}	0	3800
$H + H + H_2 O = H_2 + H_2 O$	6.00×10^{19}	-1.25	0
$H + H + H_2 = H_2 + H_2$	9.2×10^{16}	-0.6	0
$H_2 O_2 + M = OH + OH + M$	1.3×10^{17}	0	45500
$O + O + M = O_2 + M$	1.2×10^{13}	0	-1788
$H O_2 + OH = H_2 O + O_2$	7.50×10^{12}	0	0

density	2.71653 kg/m ³		
mean mol. weight	14.8652 amu		
	1 kg	1 kmol	
enthalpy	2.59574e+006	3.859e+007 J	
internal energy	436554	6.489e+006 J	
entropy	16725.2	2.486e+005 J/K	
Gibbs function	-6.19694e+007	-9.212e+008 J	
heat capacity c_p	3279.32	4.875e+004 J/K	
heat capacity c_v	2720	4.043e+004 J/K	
	Mole Fraction	Mass Fraction	Chem. Pot. / RT
H2	0.154075	0.0208942	-19.5842
H	0.0639392	0.00433541	-9.79212
O2	0.0428297	0.0921948	-30.3961
O	0.0305995	0.0329341	-15.1981
OH	0.138622	0.158598	-24.9901
HO2	0.000287541	0.000638456	-40.1881
H2O2	4.34225e-005	9.93595e-005	-49.9802
H2O	0.569603	0.690306	-34.7822

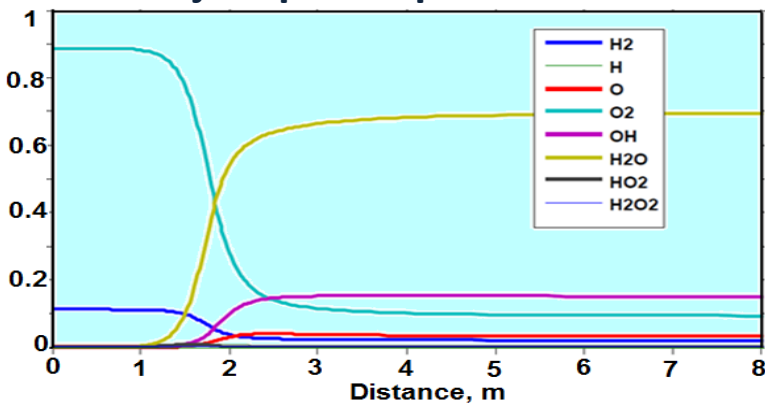
Reaction	A	b	E (cal/mol)
Hydrogen-air mechanism			
$N_2 + O = NO + N$	1.4×10^{14}	0	75800
$N + O_2 = NO + O$	6.4×10^9	1	6280
$OH + N = NO + H$	2.65×10^{16}	0	0
$N_2 + M = 2N + M$	3.7×10^{21}	-1.6	224928

Detonation wave of the H_2/O_2 stoichiometric mixture (2:1) explosion

Detonation - supersonic combustion
induced by strong shock wave
Detonation wave structure

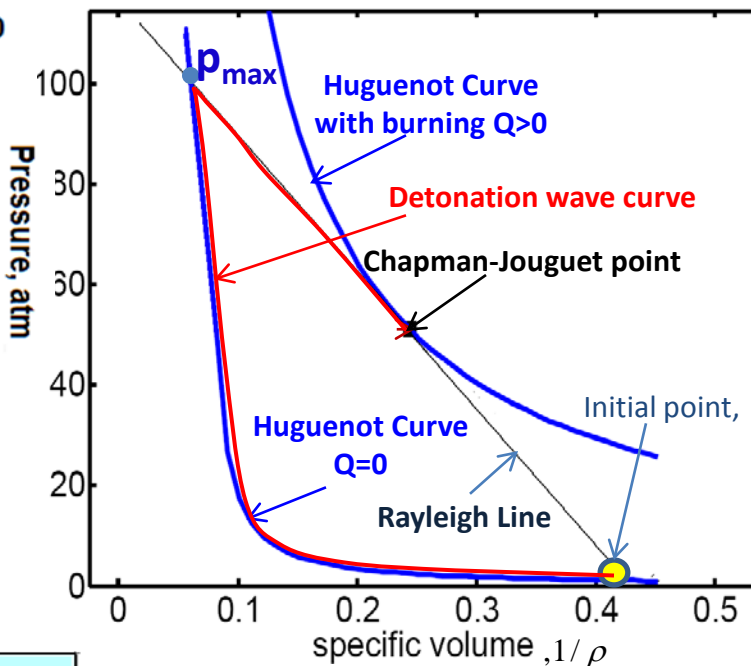


Major species profiles



Chapman–Jouguet theory, extended by
Zeldovich, Von Neumann and Doering (ZND)

Huguenot Curves and Rayleigh Line



Chapman-
Jouguet
theory

Mass, momentum,
energy conservation:

$$\rho_0 v_0 = \rho v,$$

$$p_0 + \rho_0 v_0^2 = p v^2,$$

$$c_p T_0 + \frac{v_0^2}{2} = c_p T + \frac{v^2}{2} + Q$$

With constant specific
heat assumption

$$h(T) = Q + c_p (T - T_0),$$

$$Q = \sum Y_i h_{fi}^0$$

- reaction enthalpy

Rayleigh Line:

$$P = a(1/\rho) + b$$

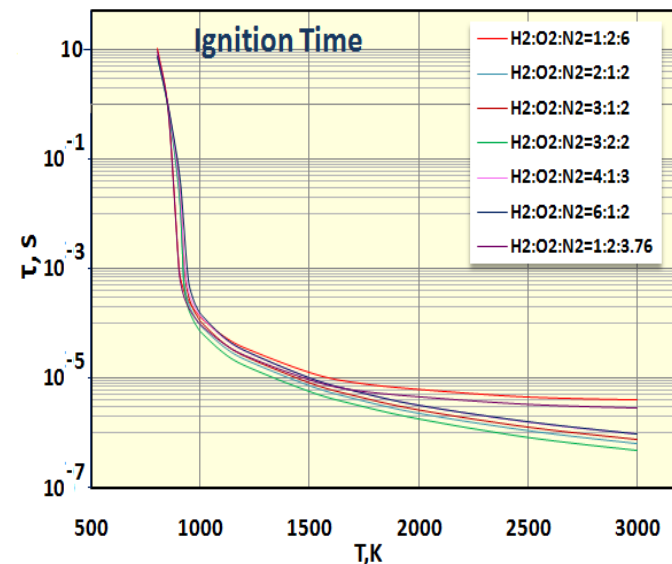
Huguenot Curve

$$\frac{\gamma}{\gamma-1} \left(\frac{p}{\rho} - \frac{p_0}{\rho_0} \right) - \frac{p-p_0}{2} \left(\frac{1}{\rho} + \frac{1}{\rho_0} \right) = Q$$



Detonation parameters of H₂/O₂/N₂ mixtures for initial mixture temperature $T_{mix} = 100K$

Compos. H ₂ :O ₂ :N ₂	2:1:4	1:2:6	2:1:2	3:1:2	3:2:2	4:1:3	6:1:2
T, K	2865	1450	3295	3261	3388	2806	2598
P _{cj} , atm	44	24	49	49	50	43	42
P _{max} , atm	82	44	92	91	94	81	76
Velocity, m/s	1972	1310	2234	2408	2278	2279	2614

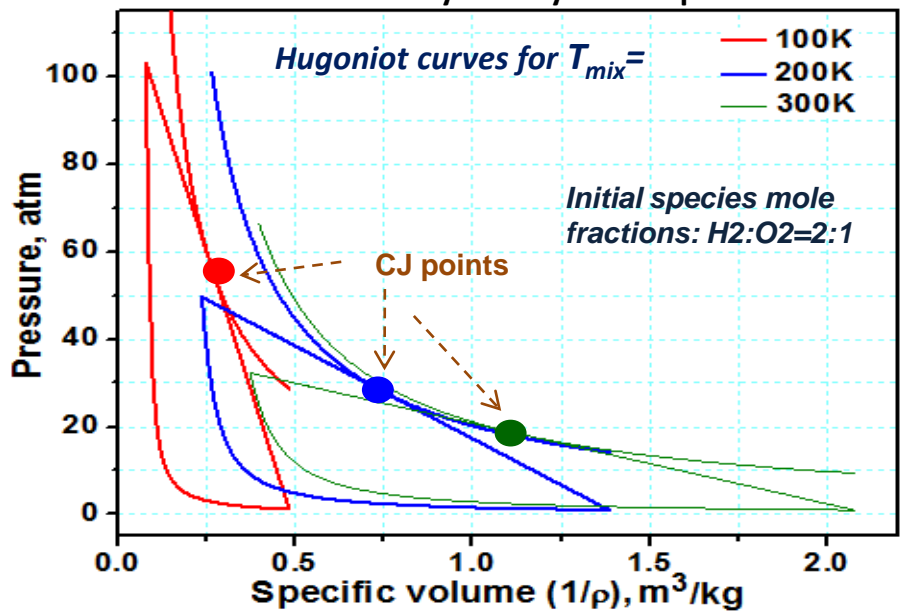


Species composition behind the detonation wave for various composition of mixture

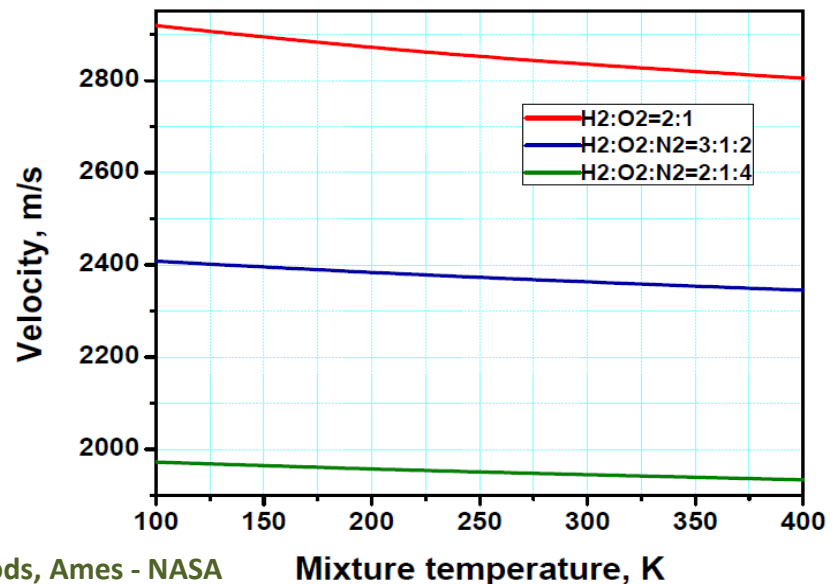
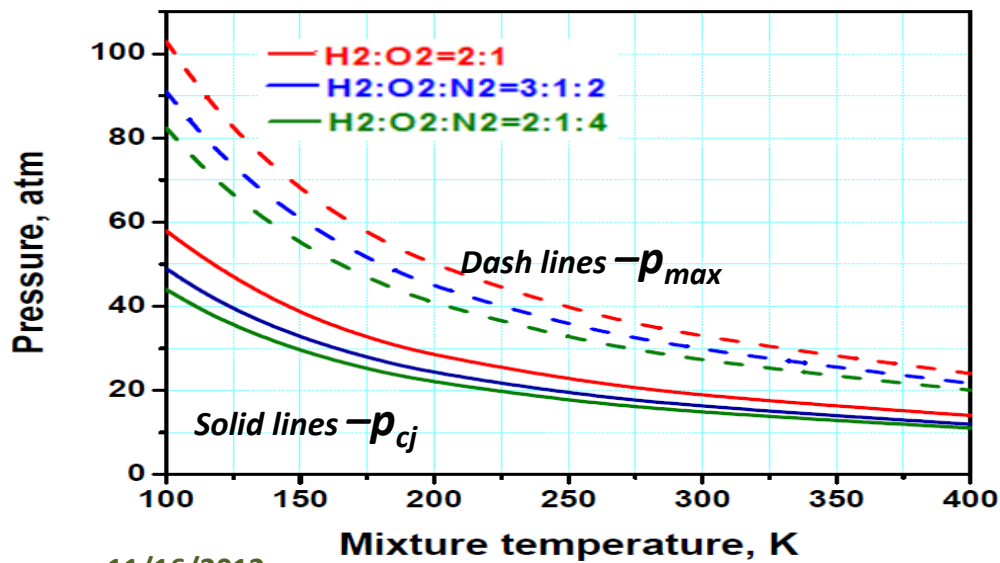
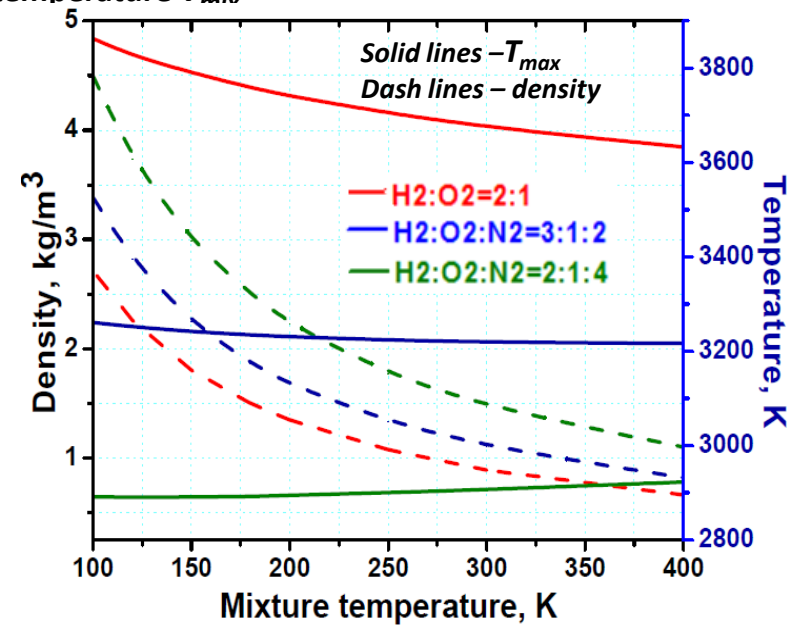
Initial compos.	2:1:4		1:2:6		2:1:2		3:1:2		3:2:2		4:1:3		6:1:2	
	Mole Fraction	Mass Fraction	Mole Fraction	Mass Fraction	Mole Fraction	Mass Fraction	Mole Fraction	Mass Fraction	Mole Fraction	Mass Fraction	Mole Fraction	Mass Fraction	Mole Fraction	Mass Fraction
H ₂	0.02	10 ⁻³	10 ⁻⁵	10 ⁻⁶	0.08	10 ⁻³	0.20	0.02	0.04	10 ⁻³	0.28	0.03	0.5	0.1
O ₂	0.01	0.01	0.18	0.2	0.02	0.03	10 ⁻³	10 ⁻³	0.08	0.11	10 ⁻⁵	10 ⁻⁴	10 ⁻⁶	10 ⁻⁶
N ₂	0.65	0.76	0.71	0.72	0.45	0.6	0.38	0.59	0.34	0.44	0.4	0.7	0.24	0.56

Nov. 5-8, 2012

Detonation pressure strongly depends on temperature T_{mix} of the mixture and relatively weakly on composition.



Detonation temperature T_{max} and velocity v_{dw} strongly depend on composition and weakly on the mixture temperature T_{mix}



11/16/2012

Detonation blast in H_2 /air mixtures accompanied by high luminescence:
high speed video frames from a detonation experiment*



10 g of C-4 high explosive was used to initiate detonation in the stoichiometric hydrogen/air mixture. The detonation velocity was 1980 m/s, which is in good agreement with the C–J detonation velocity for a stoichiometric mixture of hydrogen and air: (*M. Groethe , E. Merilo , J. Colton , S. Chiba , Y. Sato c , H. Iwabuchi., “Large-scale hydrogen deflagrations and detonations”, International Journal of Hydrogen Energy 32 (2007) 2125 – 2133.)

Conditions necessary for a detonation blast of $H_2:O_2:N_2$ mixture

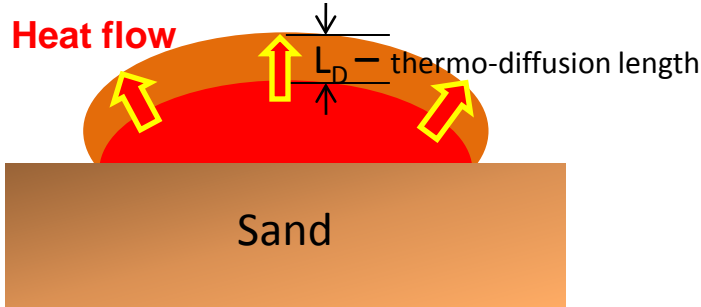
- Strong local explosion that generates a shock wave with high pressure $p > p_{\max}$.
- Critical pressure of initiating shock wave increases when radius of the localization of initiating shock wave decreases
- The critical pressure in the initiating shock wave depends on the mixture composition, periphery temperature of the mixture, and exceeds $40\text{atm} \div 100\text{atm}$.
- The formation of detonation weakly depends on temperature in the initiating shock wave.

Data of pressure sensors show that the condition $p_{\max} > 40\text{atm}$ are not fulfilled in most of the HOVI tests



Three processes determining deflagration flame dynamics:

1. Conductive heat flow from the flame front to the cold mixture. **P=1atm**

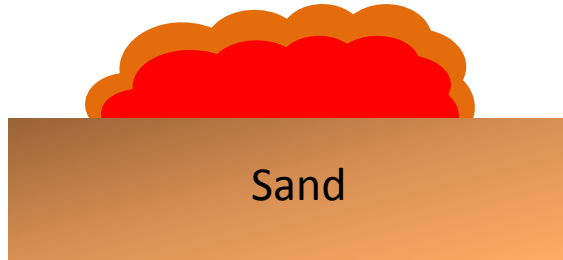


Burning rate (speed of the laminar flame in a quiescent gas)

$$v_D = \frac{L_D}{\tau_B} = \sqrt{\frac{\kappa_{air} R_b}{C_{air} \rho_{air}}} \approx (2 \div 2.5) m / sec$$

$$R_b = \tau_b^{-1} \approx 3 \times 10^5 \text{ sec}^{-1} - \text{combustion rate (see below)}$$

2. Turbulent acceleration of the burning rate according to experimental and numerical studies is:

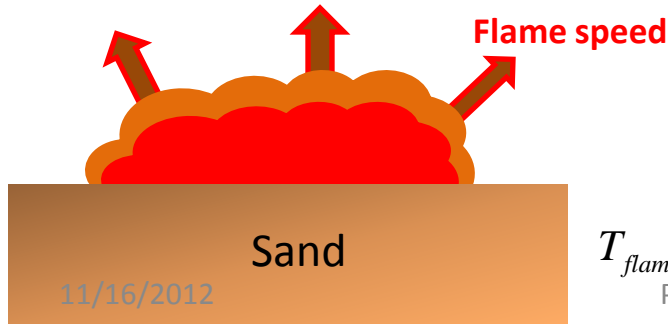


$$v_{Turb} \approx 3.6 v_D \approx (7.2 \div 9) m / sec$$

Velocity increases due to growth of effective combustion area.

V. Molkov, D. Makarov and H. Schneider, J. Phys. D: Appl. Phys. 39, 4366-4376 (2006)

3. Thermal expansion of hot combustion products and formation of fast deflagration flame at pressure close to atmospheric : $p \approx 1 \text{ atm}$.



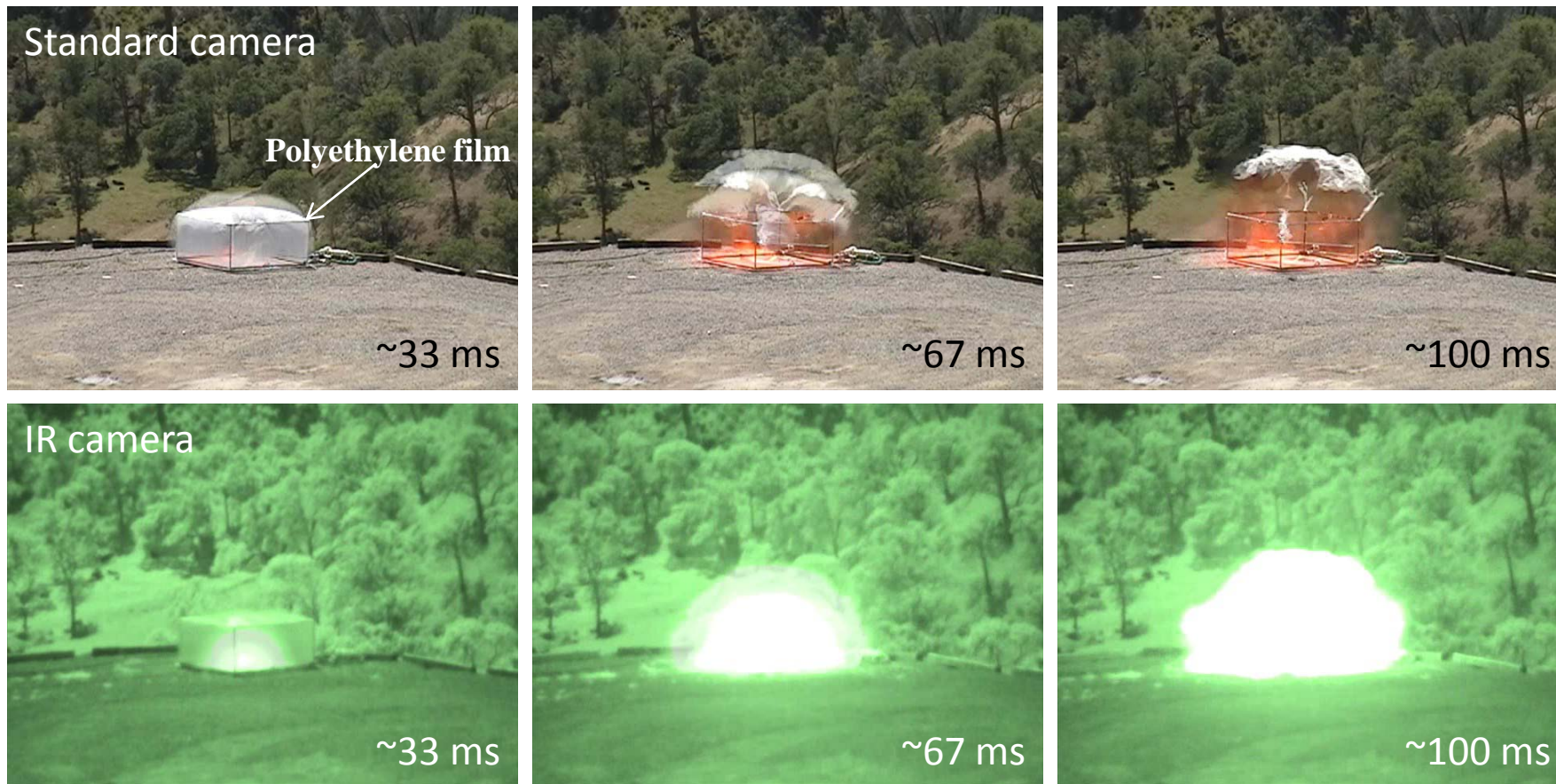
$$v_{front} \approx v_{Turb} \frac{T_{flam}}{T_{mix}} \approx (30 \div 70) m / sec$$

Flame speed increases due to expansion of hot gas (water and nitrogen) forming as a result of the combustion:

$$T_{flame} = \frac{\rho_{H_2} Q_h}{\rho_{products} C_{p, products}} + T_{atm} \approx (2800 \div 3500) K$$

Q_h - heat of combustion,
 $C_{p,v}$ - specific heat of
combustion products
 $T_{mix} = 300K$

Visible and IR pictures of an explosion of stoichiometric H₂/O₂ mixture in atmosphere*



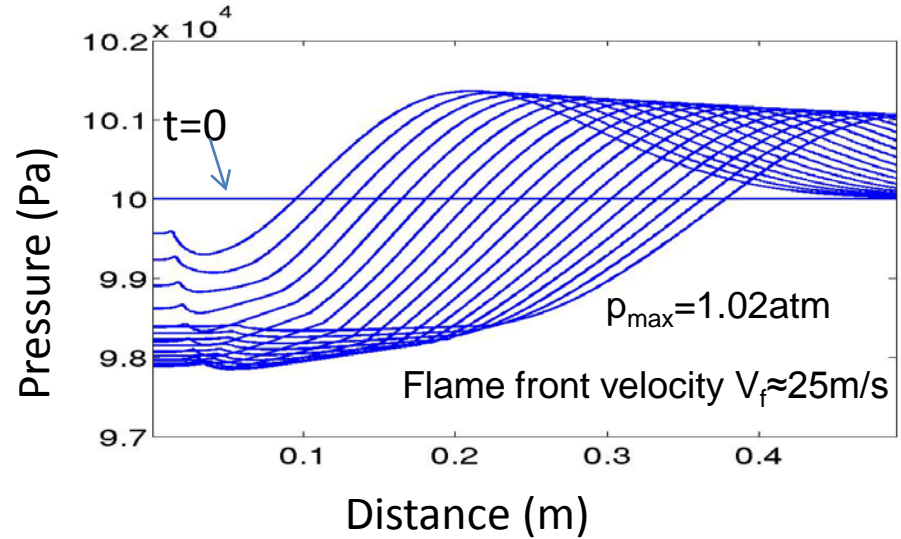
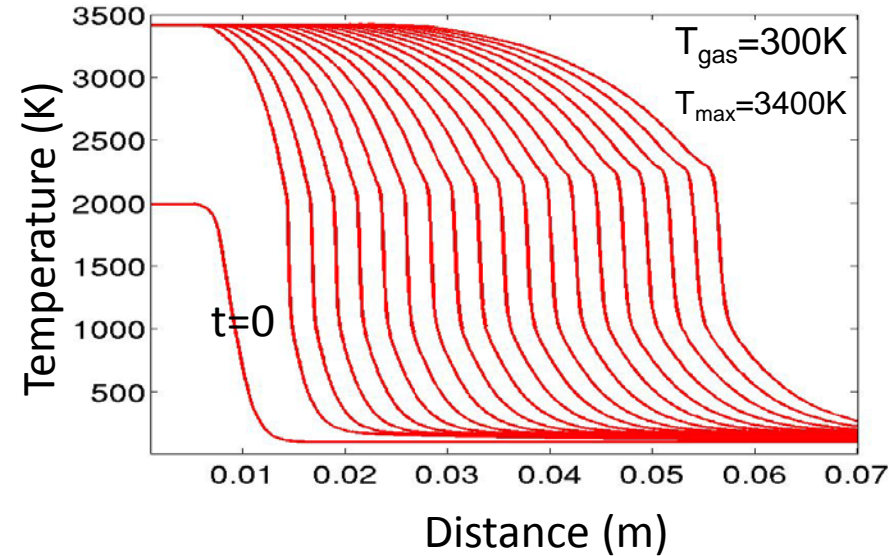
Flame front velocity $v_f = 20\text{m/sec} - 33\text{m/sec}$ for $x_{\text{H}_2} = 0.867 - 0.999$ and pressure about 1atm.

*Merilo, E.G., Groethe, M.A., "Deflagration Safety Study of Mixtures of Hydrogen and Natural Gas in a Semi-open Space",
In Proceedings of the international conference on hydrogen safety, S.Sebastian, Spain, 2007

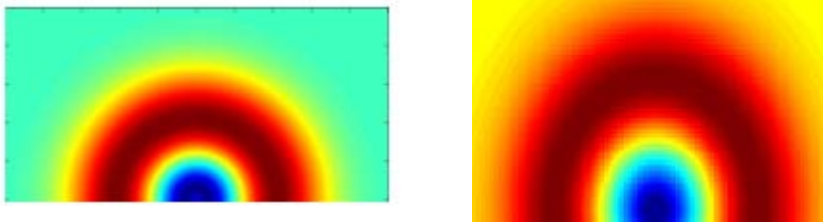
Deflagration dynamics of GH₂/GO_x/GN₂ mixture (2:1:4) (simulation results)



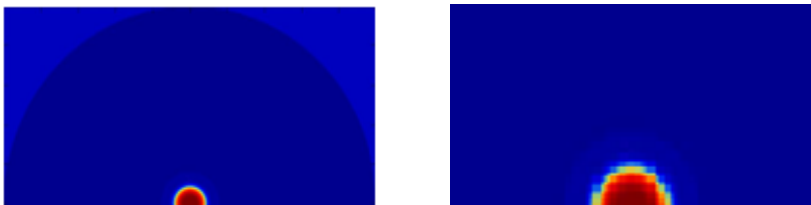
Initial conditions: $T_0=2000\text{K}$, $p_0=1\text{atm}$, and radius $R_0=1\text{cm}$



Pressure distribution for $t=0.2\text{msec}$ and $t=2\text{msec}$



Temperature distribution for $t=0.2$ and $t=2\text{msec}$



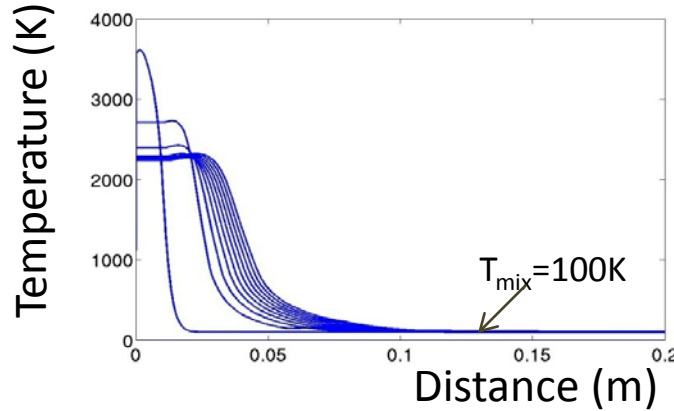
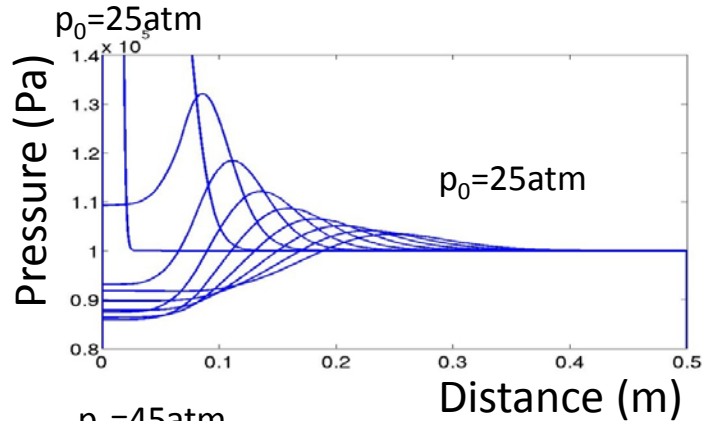
Deflagration propagates with temperature $T_{\text{max}}=3400\text{K}$, pressure $p_{\text{max}}=1.02\text{atm}$, and flame front velocity $V_f \approx 25\text{m/s}$

Pressure is very close to 1atm. The pressure length scale is much greater than that of temperature, i.e. the “temperature wave” is more localized than the “pressure wave”. Deflagration velocity is equal to

$$v_f \approx v_D \left(\frac{T_{\text{flame}}}{T_{\text{gas}}} \right) \approx 25\text{m/sec}, v_D = \sqrt{\frac{\kappa_{\text{gas}} R_b}{C_{\text{gas}} \rho_{\text{gas}}}}$$

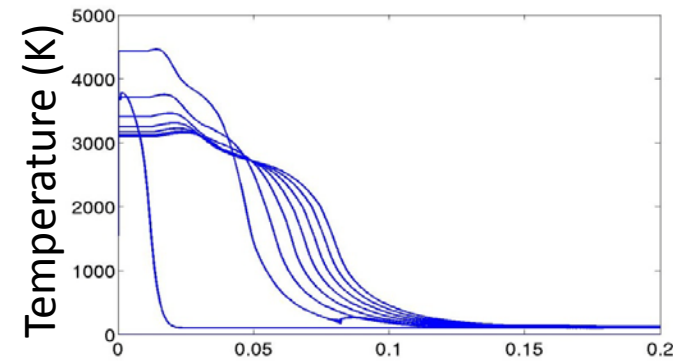
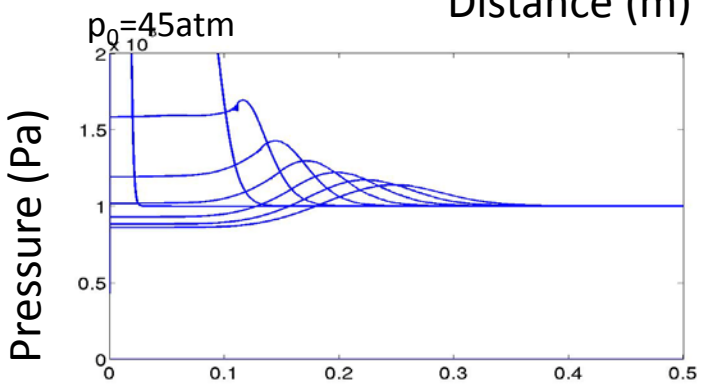
The simulation results of the simplified model agree with the results obtained from an analytical estimation.

Deflagration dynamics depending on the initial local pressure (simulation results)

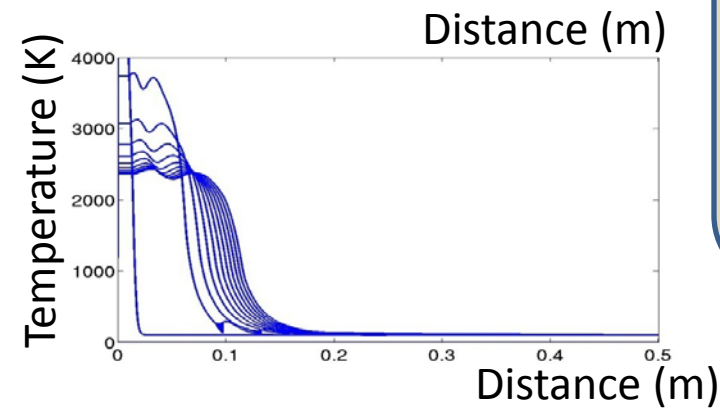
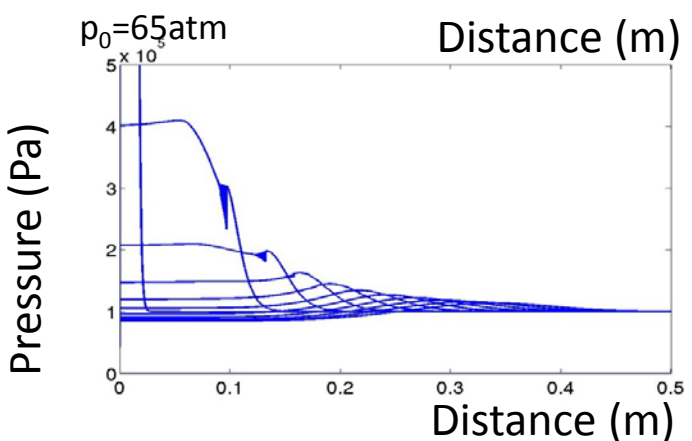


Ignition condition:
local temperature $T_0=3000\text{K}$ and pressure $p_0=25\text{atm} - 65\text{atm}$ inside area of the radius $R_0=1\text{cm}$.

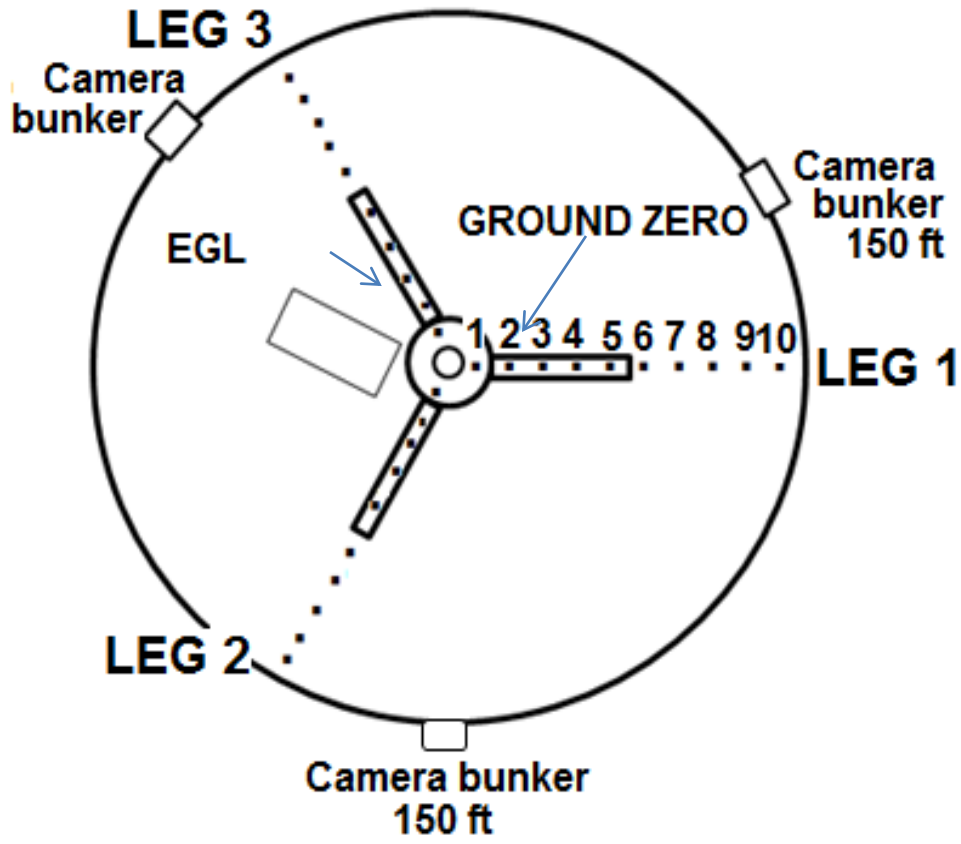
Periphery temperature of mixture $T_{\text{mix}}=100\text{K}$ and pressure $p_{\text{mix}}=1\text{atm}$



Stationary pressure, temperature and velocity of the deflagration wave are $p=1\text{atm}$, $T=2400\text{K}$, $v=30\text{m/s}$ and do not depend on the ignition conditions.



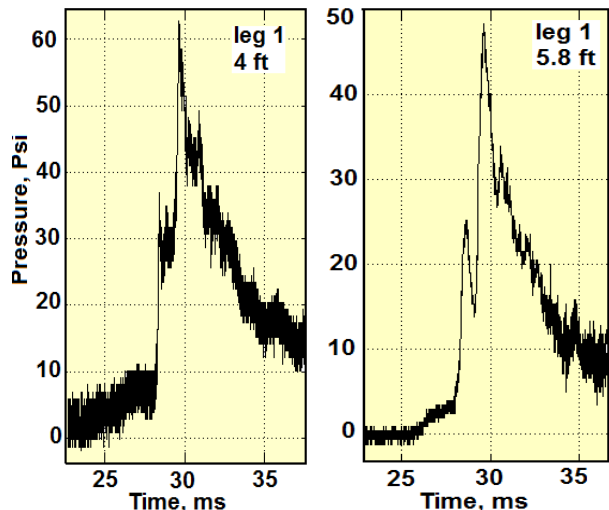
*Hydrogen/Oxygen Vertical Impact (HOVI) tests:
location of pressure sensors*



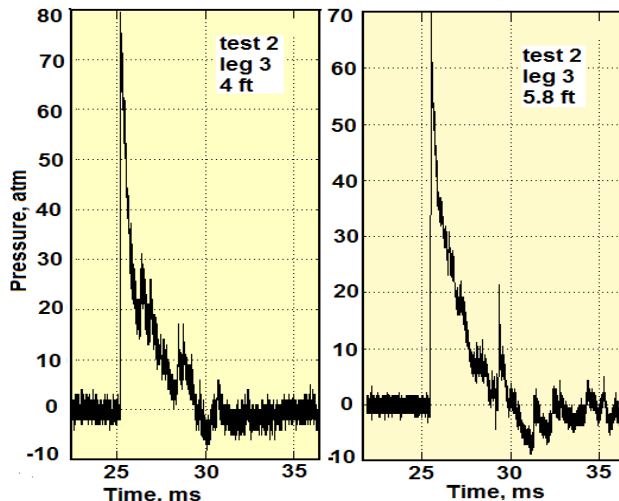
# sensor / range	1	2	3	4	5	6	7	8	9	10
ft	4	5.75	8.4	12.3	17.8	25.8	37.67	54.7	79.2	115
m	1.2	1.7	2.5	3.6	5.4	7.7	11.5	16.4	23.8	35.5

(sensor data for distances 4ft and 5.8ft from explosion center)

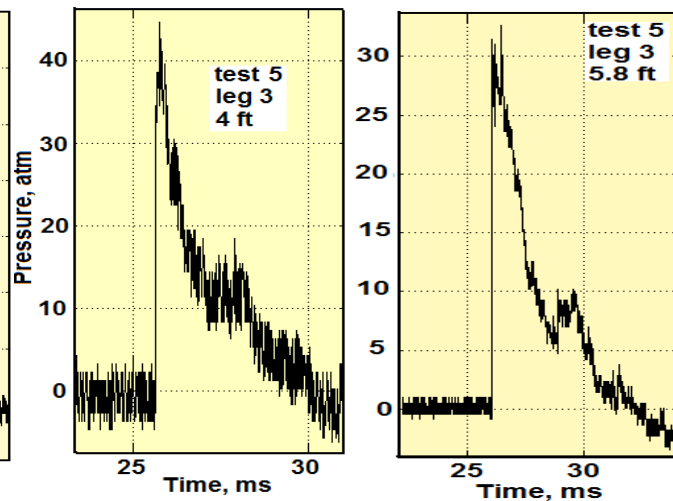
HOVI 13, $p_{max}=4.2atm$



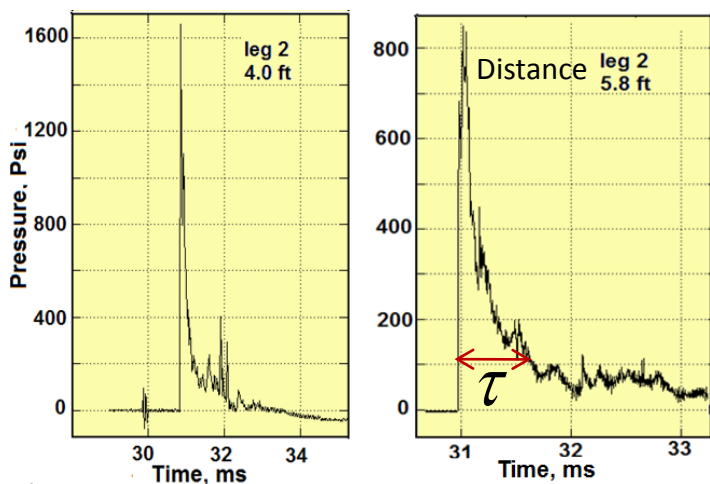
HOVI 2, $p_{max}=5.4atm$



HOVI 5, $p_{max}=3atm$



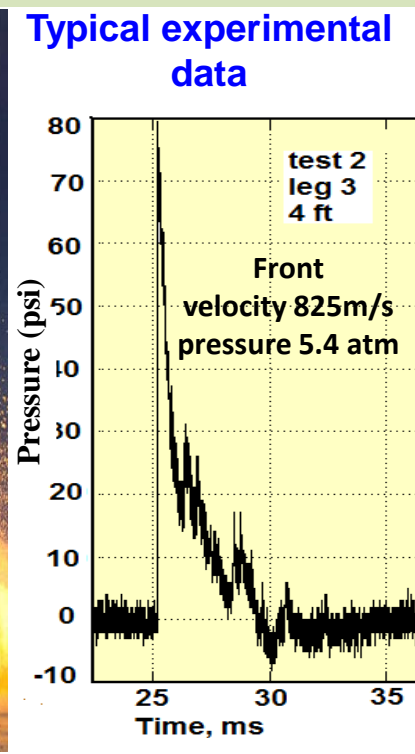
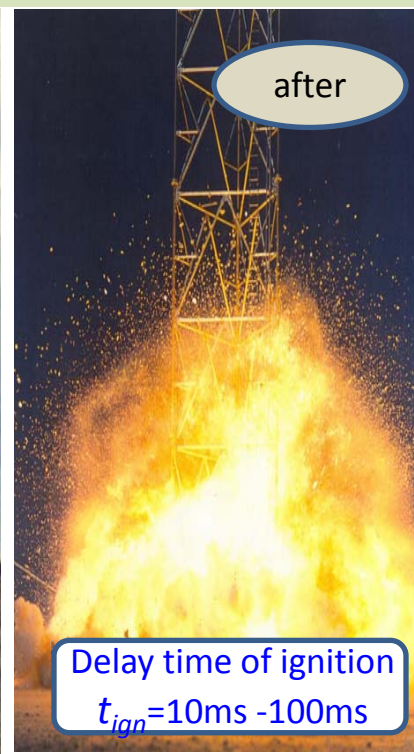
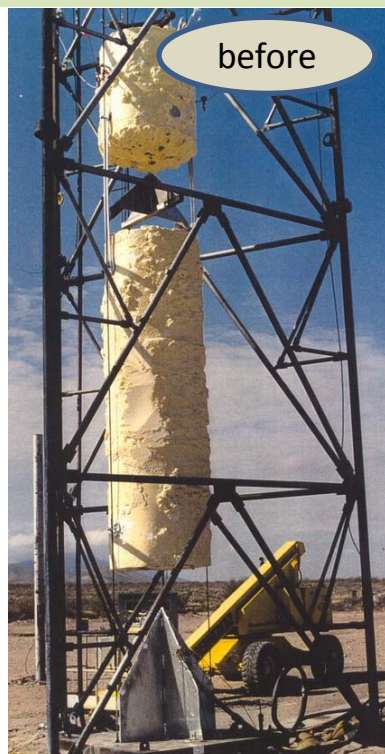
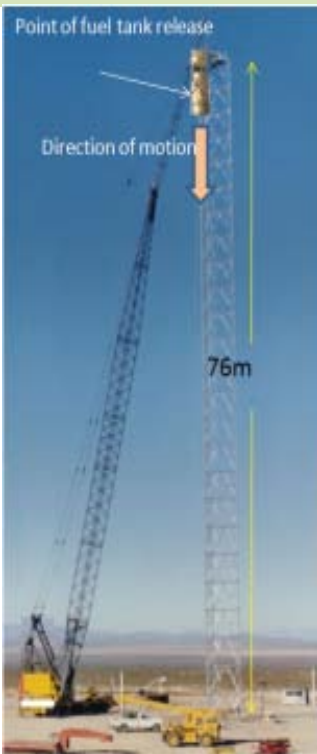
The pressure in the blast waves of all HOVI tests (except for HOVI 9) is smaller than 5.5atm, i.e. the detonation conditions are not fulfilled and the explosion is a fast deflagration.



HOVI 9, $p_{max} \approx 80atm-110atm$, $V=2966-2625m/sec$

The maximum pressure in the blast waves of HOVI 9 exceeds the critical pressure p_{max} . Such high pressure can be created by a strong shock wave of collapsing vapor bubble near LO2 surface or the formation of deflagration to detonation transition a due to aerosol combustion.

Hazards induced by breach of liquid fuel tanks: Hydrogen-oxygen vertical impact (HOVI) tests



Delay time of ignition
 $t_{ign} = 10\text{ms} - 100\text{ms}$

HOVI test	Pressure data, atm	Experimental shock velocity, m/sec (different directions)	Duration of shock wave msec
13	4.46 ÷ 5.4	740 ÷ 825	~ 3.5
5	2.5 ÷ 3	620 ÷ 660	~ 4.0
2	3.2 ÷ 4.7	730 ÷ 780	~ 3.4
9	80 ÷ 110	2625 ÷ 2966	~ 0.7

Outstanding problems:

(i) HOVI tests showed that cryogenic H₂/O_x mixtures *always self-ignite* without any external sources when gaseous hydrogen and oxygen mix with a liquid O_x stream; *Source of self-ignition was enigmatic!*

(ii) HOVI tests data (pressure $p_f \sim 5\text{atm}$ and velocity $v_f \sim 600\text{m/s}$ of explosion front) cannot be explained by existent theory of detonation ($p_f > 50\text{atm}$, $v_f > 2000\text{m/s}$) and deflagration ($p_f = 1\text{atm}$, $v_f < 30\text{m/s}$).

Key differences between the HOVI test data and the conventional deflagrations

- High speed in excess of **700 m/sec**
- Relatively high pressure of the blast waves **from 3 atm to 5 atm (>100atm for HOVI 9)**
- High luminescence accompanying the blast

Conclusions about ignition conditions from HOVI tests

- Ignition always occurred in the LH2/LO2 pan tests. Tests demonstrated that this ignition is not due to external sources.
- The HOVI tank test data later verified the tendency for self-ignition of liquid hydrogen and liquid oxygen, because each HOVI test ignited without external assistance.
- The HOVI test data also showed that a liquid hydrogen spill alone is not likely to self-ignite, because in every HOVI test with a ground cloud of hydrogen, caused by a breach in the bottom of the hydrogen tank, the ground cloud did not ignite until liquid oxygen was released.
- HOVI test data showed that the ignition occurs when gaseous hydrogen (GH₂) and oxygen (GO_x), and liquid oxygen (LO_x) mixture is available.

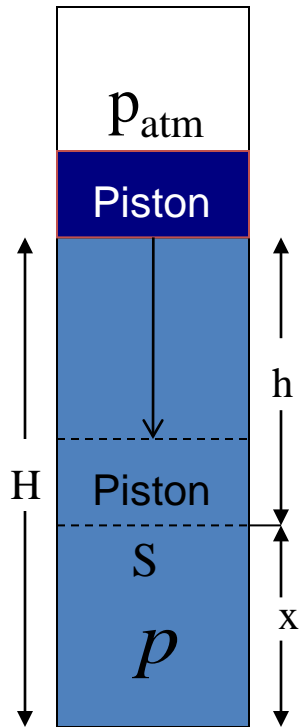
The **cavitation-induced mechanism** of ignition can arise just when gaseous hydrogen (GH₂) and oxygen (GO_x), and liquid oxygen (LO_x) mixture is available.

Cavitation is collapse of oscillating bubbles of vapor GO_x in LO_x.

Cavitation-induced ignition of H₂/O_x mixtures is determined by injection of super-heated and super-compressed gas formed in a bubble collapsing near the LO_x surface into the space above LO_x surface and ignition of the GH₂/GO_x mixture in this space.

The ignition effect intensifies when GH₂ is inside the collapsing vapor bubble in LO_x.

The cavitation ignition is a random process that is characterized by different maximum temperature and pressure of gases injected from the collapsing bubble in gaseous H₂/O₂ mixtures.



A simple analogy of this effect is inertial adiabatic compression of a gas in a cylinder under the action of the piston. In this case

$$\frac{p}{p_0} = \left(\frac{V_0}{V}\right)^\gamma = \left(\frac{H}{x}\right)^\gamma; \quad \frac{T}{T_0} = \left(\frac{V_0}{V}\right)^{\gamma-1} = \left(\frac{H}{x}\right)^{\gamma-1}$$

and the equation of motion of piston of mass M is

$$M\ddot{h} = Mg + p_{atm}S - pS; \quad h = H - x$$

$$\frac{M}{S}\ddot{x} = p_0\left(\frac{H}{x}\right)^\gamma - p_L; \quad p_L = p_{atm} + \frac{Mg}{S}$$

Initial condition: $t = 0 \quad \dot{x} = v = 0 \quad x = H$

Final condition: $t = t_f \quad \dot{x} = v = 0 \quad x = x_{min}$
 p_0 is initial vapor pressure.

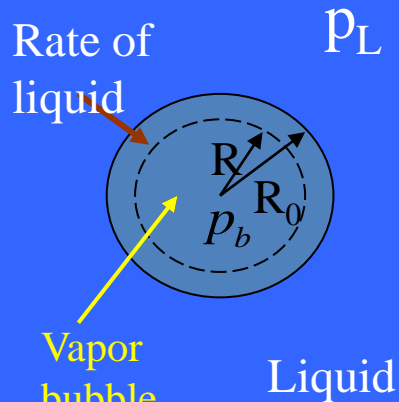
Solution for $p_0 \ll p_a$

$$x_{min} = H \left(\frac{p_0}{(\gamma-1)p_L} \right)^{\frac{1}{\gamma-1}}$$

$$\Gamma = (\gamma-1)^{\frac{\gamma}{\gamma-1}} \quad \gamma = \frac{C_p}{C_v} = 1.4$$

$$p_{max} = p_L \Gamma \left(\frac{p_L}{p_0} \right)^{\frac{1}{\gamma-1}},$$

$$T_{max} = T_0 \left(\frac{(\gamma-1)p_L}{p_0} \right)$$



Effect of strong compression of vapour bubble and initiation of extremely high temperature and pressure in it is determined by inertia of the heavy piston motion.

The role of the piston in cavitation of a vapor bubble is played by the liquid. The effect intensifies due to the condensation and burning of GOx/ GH2 mixture inside the bubble

If the initial gas temperature $T_0=300K$ and pressure $p_0 < 0.1p_a$ then the maximum pressure and temperature in both the piston and the collapsing bubble are

$$p_{max} \geq 125atm$$

$$T_{max} \geq 1200K$$



(a) Without considering condensation

Rayleigh-Plesset equation of bubble motion

$$R \frac{d^2 R}{dt^2} + \frac{3}{2} \left(\frac{dR}{dt} \right)^2 + \frac{4\nu}{R} \frac{dR}{dt} + \frac{2\sigma}{\rho_L R} = \frac{p_b(R) - p_L}{\rho_L}$$

$$p_b(R) = p_0 \left(R_0 / R \right)^{3\gamma}, \quad p_L^* = p_L + 2\sigma / R_0$$

$$R_{\min} \approx R_0 \left(\frac{p_0}{(\gamma-1)p_L^*} \right)^{\frac{1}{3(\gamma-1)}}$$

$$p_{\max} = \Gamma p_L \left(\frac{p_L^*}{p_0} \right)^{\frac{1}{(\gamma-1)}}, \quad T_{\max} = T_0 \left(\frac{(\gamma-1)p_L^*}{p_0} \right)$$

p_0 is initial pressure of the neutral gas.

Initial LOx temperature $T_0 = 90K$ and pressure $p_0 = 1atm$. The overpressure shock jump is $0.5atm$ ($p_L - p_0 = 0.5atm$), then the maximum vapor pressure and temperature in the collapse bubble are

(a) without considering of condensation:

$$\Delta p_{\max} \approx 0.017atm \quad \Delta T_{\max} \approx 54K$$

(b) With considering of condensation

The Ox vapor bubble contains saturated oxygen vapor and a small portion of gaseous hydrogen (GH2). p_v is pressure of saturated oxygen vapor, p_{g0} is initial GH2 pressure: $p_{g0} \ll p_v$. The saturated vapor condenses on the bubble wall and its pressure remains low down to a very small radius for $t < t_c$.

$$p_b(t) = p_v + p_{g0} \left(R_0 / R \right)^{3\gamma}, \quad p_v \ll p_{g0}$$

$$p_b(t) \ll p_v \quad \text{at} \quad t < t_c = \left(R_0 / \Sigma \right)^{2/3} \propto \left(\rho_L / \rho_v \right)^{4/3}$$

$$\Sigma(T_L) = \frac{q_L^2}{c_L T_L D_L^{1/2}} \left(\frac{\rho_v}{\rho_L} \right)^2 \quad t_f = 0.915 \left(\frac{\rho_L R_0^2}{p_L - p_v} \right)^{1/2} \quad \text{Time of bubble collapse}$$

$\approx 4 \times 10^{-4} \text{ sec for } R_0 \approx 1mm$

- thermodynamic parameter

$$t_c = \left(R_0 / \Sigma \right)^{2/3} < t_f$$

This is condition of the effect: condensation is intensive enough.

It is valid for LOx but not for LH2 due to different of T_L and relation (ρ_L / ρ_v)

$$p_{\max} \approx p_{g0} \left(\frac{(\gamma-1)p_L^*}{p_{g0}} \right)^{\frac{\gamma}{(\gamma-1)}}, \quad T_{\max} \approx T_0 \left(\frac{(\gamma-1)p_L^*}{p_{g0}} \right)$$

$$R_{\min} \approx R_0 \left(\frac{p_{g0}}{(\gamma-1)p_L^*} \right)^{\frac{1}{3(\gamma-1)}}, \quad p_L^* = p_L - p_v + 2\sigma / R_0$$

(b) with considering of condensation for $p_L - p_0 = 0.5atm$:

$$p_{\max} \approx 300(800)atm \quad T_{\max} \approx 5400(11000)K,$$

$$R_{\min} \approx 0.03(0.02)mm \quad \text{for } p_{g0} = 0.01(0.005)atm$$

Equations for radius of the collapsing vapor bubble in liquid

For the incompressible liquid $\frac{\partial \rho_L}{\partial t} = 0 \Rightarrow \frac{\partial}{\partial r}(\rho_L u_L) + \frac{2\rho_L u_L}{r} = 0$

Using the boundary condition $\left[\rho_L (u_L - \dot{R}) \right]_R = -j_{cd}$ we find:

$$u_L(r, t) = \left(\frac{R}{r} \right)^2 \dot{R} - \frac{j_{cd}}{\rho_L} \left(\frac{R}{r} \right)^2$$

Then the conservation moment equation

$$\frac{\partial u}{\partial t} + u \frac{\partial u}{\partial r} = -\frac{1}{\rho} \frac{\partial p}{\partial r} + \frac{\mu}{\rho} \Delta u$$

can be written as

$$-\frac{1}{\rho_L} \frac{\partial p_L}{\partial r} = \ddot{R} \left(\frac{R}{r} \right)^2 + \frac{2R}{r^2} \dot{R}^2 - \frac{1}{\rho_L} \left(\frac{R}{r} \right)^2 \frac{dj_{cd}}{dt} - \frac{2j_{cd}R\dot{R}}{\rho_L r^2} - \frac{2R^4}{r^5} \dot{R}^2 + \frac{2j_{cd}R^4}{\rho_L r^5} \dot{R} + \frac{2R^4}{r^5} \frac{j_{cd}\dot{R}}{\rho_L} - \frac{j_{cd}^2}{\rho_L^2} \frac{2R^4}{r^5}$$

Integrating this equation from R and taking into account boundary condition for the pressure at $r=R$ is

$$p_L + \frac{2\sigma}{R} = p_m + \frac{j_{cd}^2 \rho_m (\rho_L - \rho_1)}{\rho_L \rho_1^2} - \frac{2\mu}{3R} \left(\dot{R} - \frac{j_{cd}}{\rho_L} \right)$$

we obtain the modified Rayleigh-Plesset equation for the bubble radius:

$$\ddot{R}R + \frac{3}{2}(\dot{R})^2 - \dot{R} \frac{j_{cd}}{\rho_L} - \frac{R}{\rho_L} \frac{dj_{cd}}{dt} - \frac{j_{cd}^2}{2\rho_L^2} = -\frac{p_L}{\rho_L} + \frac{p_m}{\rho_L} - \frac{2\sigma}{R\rho_L} + \frac{j_{cd}^2 \rho_m (\rho_L - \rho_1)}{\rho_L^2 \rho_1^2} - \frac{2\mu}{3R\rho_L} \left(\dot{R} - \frac{j_{cd}}{\rho_L} \right)$$

A high-fidelity model of collapsing of Ox vapor bubbles with admixed GH2 taking into consideration the burning inside the bubble was developed. The equations for the incompressible liquid phase ($r > R(t)$) may be reduced to the equation for the bubble radius R :

$$R \frac{d^2 R}{dt^2} + \frac{3}{2} \left(\frac{dR}{dt} \right)^2 + \frac{j_{cd}}{\rho_L} \frac{dR}{dt} + \frac{R}{\rho_L} \frac{dj_{cd}}{dt} = \frac{p_m - p_L}{\rho_L} - \frac{2\sigma}{R\rho_L} + \frac{j_{cd}^2 (2\rho_L - \rho_m)}{2\rho_L^2 \rho_m} - \frac{4\mu}{R\rho_L} \left(\dot{R} - \frac{j_{cd}}{\rho_L} \right)$$

the advection-diffusion equation for the liquid temperature T_l :

$$\frac{\partial T_l}{\partial t} + \left(\frac{R}{r} \right)^2 \left(\frac{dR}{dt} + \frac{j_{cd}}{\rho_L} \right) \frac{\partial T_l}{\partial r} = \frac{\kappa_L}{C_L \rho_L r^2} \frac{\partial}{\partial r} \left(r^2 \frac{\partial T_l}{\partial r} \right)$$

with initial and boundary conditions:

$$R(t=0) = R_0, \dot{R}(t=0) = 0, T_L(0) = T_m(0) = T_{L0}, T_L(r \rightarrow \infty) = T_{L0}, (T_L(r=R) = T_m(r=R) = T_s).$$

Due to high gas temperature in the bubble the equations for gas phase are:

$$p_{H_2} = c_{H_2} R_0 T_m, p_{O_x} = c_{O_x} R_0 T_m,$$

$$p_{H_2O} = c_{H_2O} R_0 T_m,$$

$$p_m = R_0 T_m \sum_i c_i = R_0 T_m c_m$$

$$\frac{\partial E}{\partial t} + \frac{1}{r^2} \frac{\partial}{\partial r} \left(r^2 u_m (p_m + E) \right) = \frac{1}{r^2} \frac{\partial}{\partial r} \left(r^2 \kappa_m \frac{\partial T_m}{\partial r} \right) + Q_h G_{comb}$$

$$E = \frac{5}{2} R_0 T_m c_m + \frac{1}{2} \rho_m u_m^2, \quad \rho_i = c_i M_i, \quad \rho_m = \sum_i c_i M_i,$$

$$\frac{\partial u_m}{\partial t} + u_m \frac{\partial u_m}{\partial r} = - \frac{R_0}{\rho_m} \frac{\partial (T_m c_m)}{\partial r}, \quad \kappa_m = \sqrt{\frac{T_m}{T_0}} \sum \frac{c_i}{c_m} \kappa_i(T_0)$$

j_{cd} is condensation-evaporation Ox flow given by the well-known Hertz-Knudsen equation:

$$j_{cd} = \frac{\beta (p_{O_x} - p_s(T_s))}{\sqrt{2\pi R_{O_x} T_s}}, \quad p_s(T_s) = p_c \left(\frac{T_s}{T_c} \right)^\lambda$$

p_s - saturation vapor pressure, R_{O_x} is vapor constant, $\beta \leq 1$ is the accommodation coefficient, $\lambda = 7$

Here r is the radial coordinate, ρ_L , C_L and r_L are the liquid density, specific heat and thermal conductivity, p_m and ρ_m are the pressure and gas mass density, respectively, p_L is pressure in liquid far from the bubble; R_0 , c_i are the gas constant and mole concentration i - gas; ρ_m , T_m , u_m , and E are the total density, temperature, velocity, and energy of gas mixture (H2, O2, H2O).

Dynamics of the gas mixture inside a bubble, taking into account the combustion and high diffusivity of the light GH2 molecules, can be written as

$$\frac{\partial c_{Ox}}{\partial t} + \frac{1}{r^2} \frac{\partial}{\partial r} (r^2 c_{Ox} u_m) = -\frac{1}{2} G_{comb}, \quad \frac{\partial c_{H_2O}}{\partial t} + \frac{1}{r^2} \frac{\partial}{\partial r} (r^2 c_{H_2O} u_m) = G_{comb},$$

$$\frac{\partial c_{H_2}}{\partial t} + \frac{1}{r^2} \frac{\partial}{\partial r} (r^2 c_{H_2} u_m) + G_{comb} = \frac{1}{r^2} \frac{\partial}{\partial r} \left[r^2 D_{H_2} \left(\frac{\partial c_{H_2}}{\partial r} - \frac{c_{H_2}}{2T_m} \frac{\partial T_m}{\partial r} \right) \right]$$

Here

$$D_{H_2} = \left(\frac{T_m}{T_0} \right)^{3/2} \left(\frac{P_0}{P_m} \right) D_{H_2}(T_0, P_0)$$

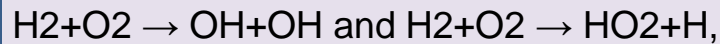
is hydrogen diffusion coefficient.

q_h is the latent heat of vaporization

The initial and boundary conditions for above equations are:

$$\frac{\partial T_m}{\partial r} \Big|_{r=0} = 0, \quad \left(\kappa_m \frac{\partial T_m}{\partial r} - \kappa_l \frac{\partial T_l}{\partial r} \right) \Big|_{r=R} = j_{cd} q_h, \quad \frac{\partial c_i}{\partial r} \Big|_{r=0} = 0, \quad c_i \Big|_{r=0} = c_i^0, \quad u_m \Big|_{r=0} = 0, \quad u_m \Big|_{r=R} = \frac{\partial R}{\partial t} - \frac{j_{cd}}{c_{Ox} M_{Ox}}, \quad \frac{j_{cd} c_{H_2}}{c_{Ox} M_{Ox}} = D_{H_2} \left(\frac{\partial c_{H_2}}{\partial r} - \frac{c_{H_2}}{2T_m} \frac{\partial T_m}{\partial r} \right) \Big|_{r=R},$$

The burning of GOx/GH2 mixture is described by 20 chain chemical reactions in CANTERA CODE that include generation of O, H, OH species. For simplicity here we consider a simplified model of the burning that takes into account only main gas components that can arise in a collapsing bubble (at $0 < r < R$): oxygen vapor, non-condensable gaseous hydrogen and water generated as a result of the burning. The simplified model based on the assumption that the burning rate is limited by the initiation reactions having the lowest rates:



Thus, we modeled the GH2/GOx combustion by the brutto reaction $H_2 + O_2 \rightarrow H_2O + 1/2 O_2$ with the rate: (T is in degrees Kelvin).

$$G_{comb} = c_{H_2} c_{Ox} [1.1 \cdot 10^8 \exp(-19680 / T) + 1.48 \cdot T^{2.433} \exp(-26926 / T)] m^3 / mol / s$$

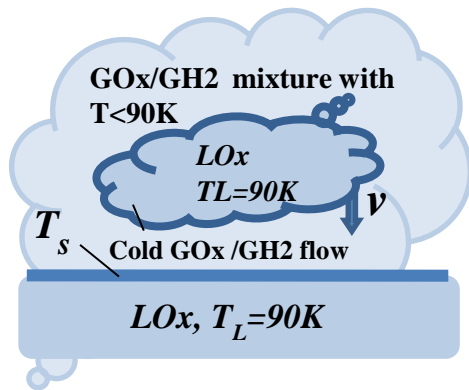
This simplified combustion model predicts the same parameters of steady detonation and deflagration waves as those obtained with the help of the full model describing all main chain reactions of GOx/GH2 mixture combustion.

An algorithm and a computer code were developed.

The algorithm uses MUSCL scheme with variable mesh that is thinner near the gas/liquid boundary. We use variable time-step algorithm that is applicable to stiff problems.

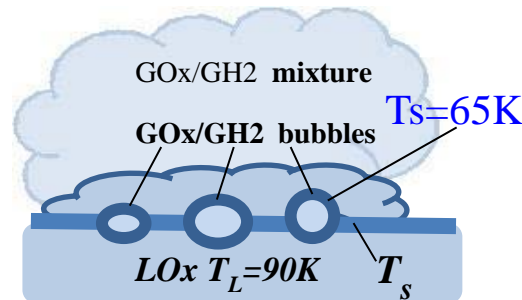
Cooling of surface of O₂/H₂ bubbles, their collapse and generation of a strong shock wave

(1) Cooling of surface of LOx fragments by cold GH₂



Over 30 msec ignition delay time
0,1 mm surface layer of LOX fragment submerged into ~ 30K GH₂ atmosphere will be cooled down to 60K - 70K.

(2) Formation of bubbles with thin cooled liquid layers and low pressure

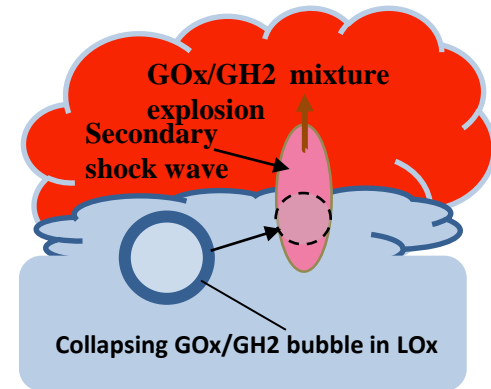


$$p = p_c \left(\frac{T_s}{T_c} \right)^7$$

$$T_c = 154.6K \quad p_c = 50.4\text{atm}$$

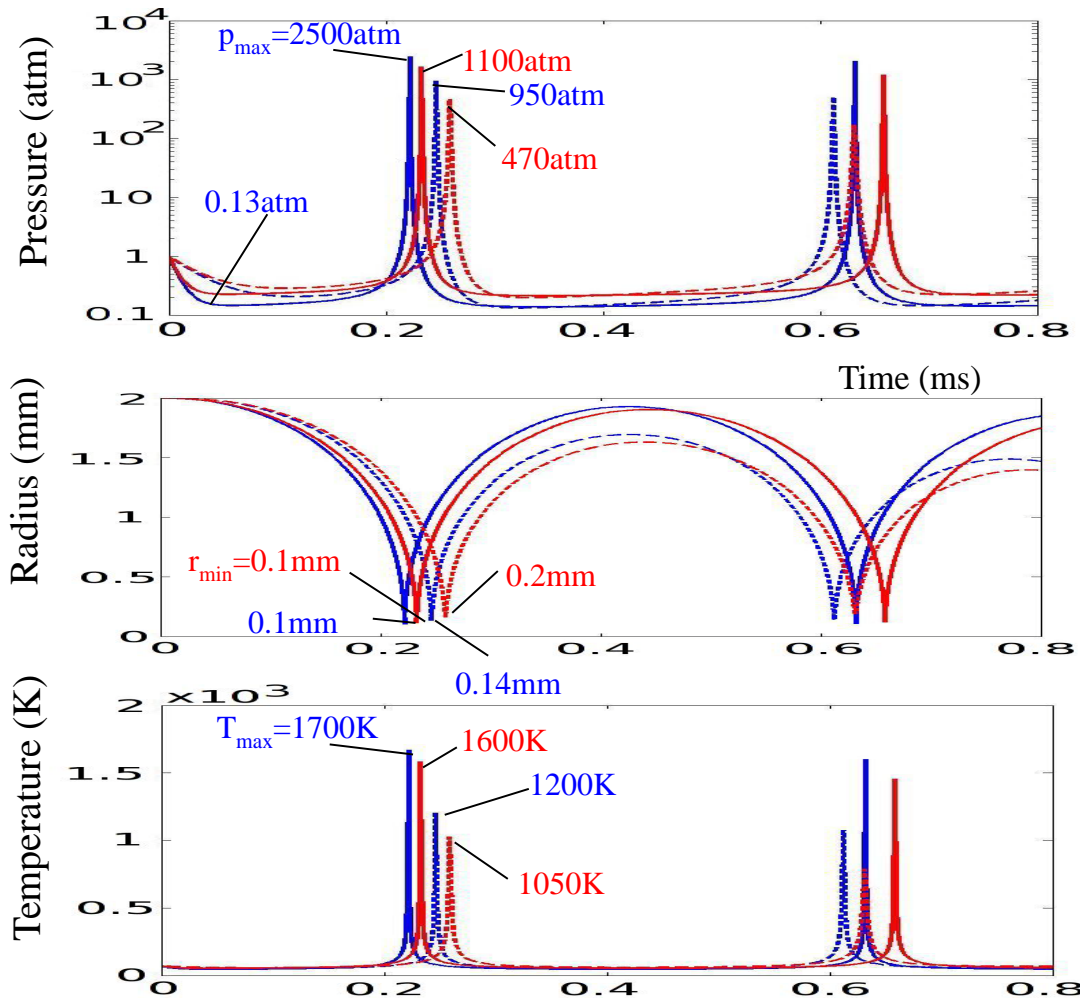
$$p = 0.12\text{atm at } 65K$$

(3) Collapse of the bubble and generation of the strong shock wave by the bubble collapsing near the liquid-gas interface.



Simulation results (scenario 1):

Formation of collapsed bubble with *gigantic pressure and temperature*



Code based on high-fidelity physics-based complex model for collapsing bubble was developed. The model takes into account the dynamic condensation-evaporation processes and combustion of O_x/H₂ mixture inside the bubble.

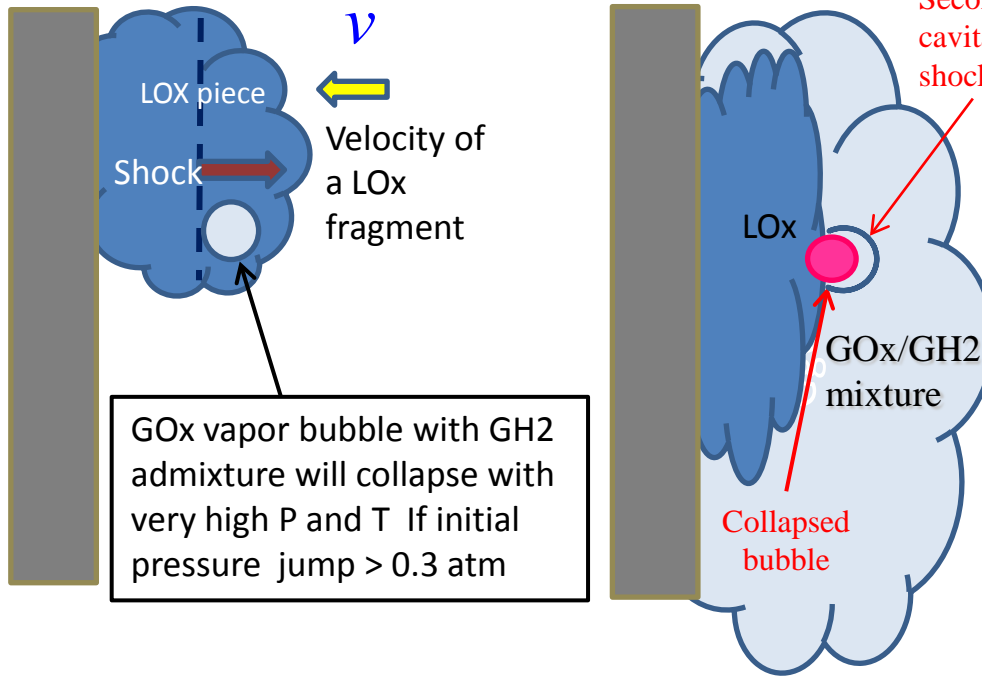
An algorithm and a computer code were developed.

The algorithm MUSCL scheme with variable mesh that is thinner near the gas/liquid boundary. We use variable time-step algorithm that is applicable to stiff problems.

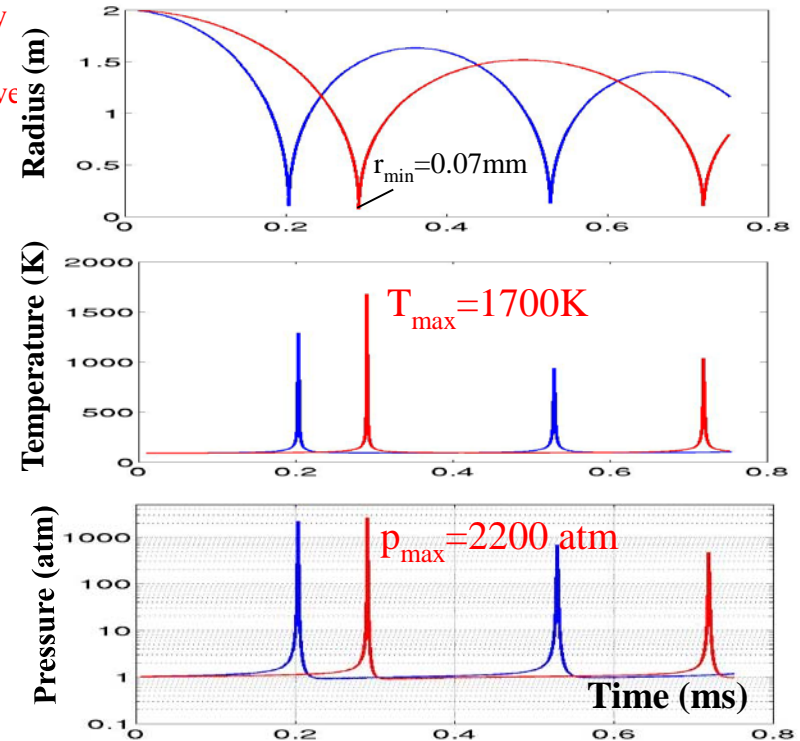
Collapsing of bubble of radius $r_0 = 2 \text{ mm}$, surface temperature $T_s = 65 \text{ K}$ (blue) and 70 K (red), ambient pressure $p = 1 \text{ atm}$, and initial partial GH₂ pressure 0.01 atm for different Hertz-Knudsen accommodation coefficient $\alpha = 1$ (solid) and 0.3 (dashed).

Scenario 2: Formation in a LOx fragment of a "weak" shock producing of vapour bubble collapsing and cavitation-induced ignition of GH2/Ox mixture

Model of formation of a "weak" shock as a result of impact of a LOx piece on a solid wall



After the impact, the weak shock wave induces collapse of bubble near the liquid- mixture interface (result simulation).



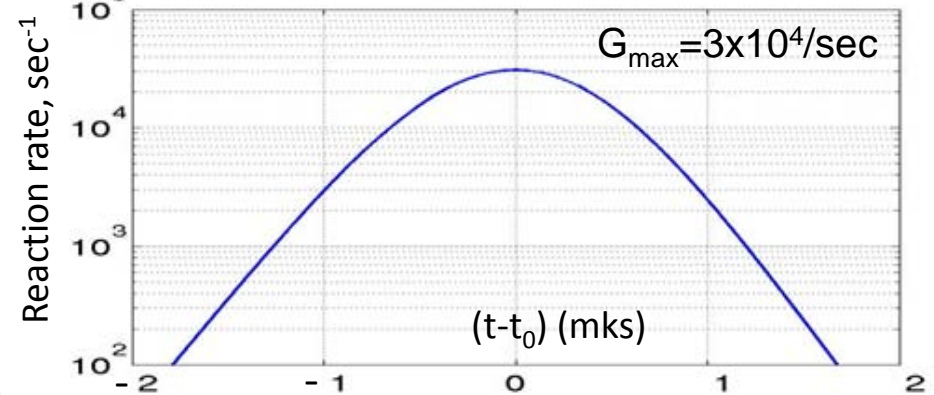
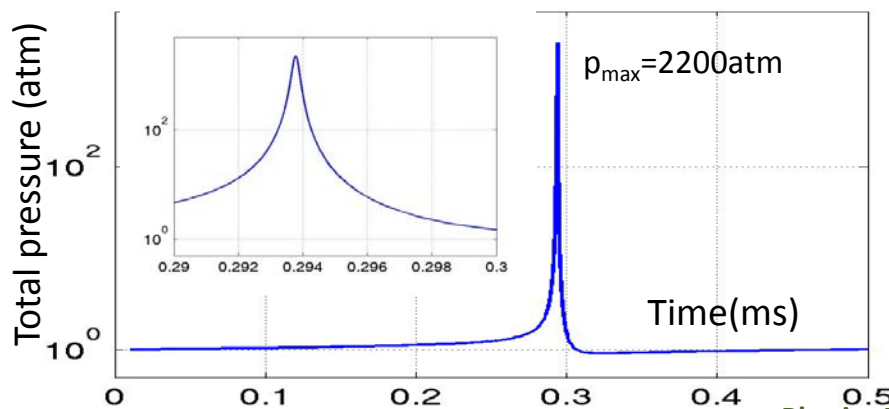
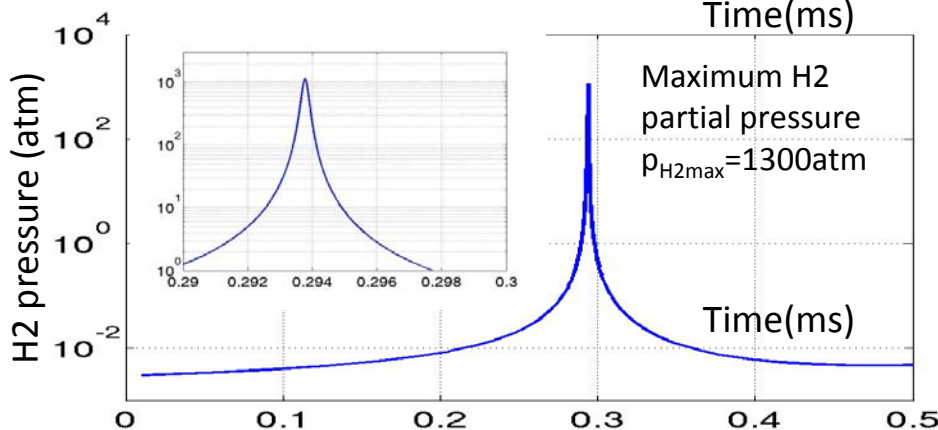
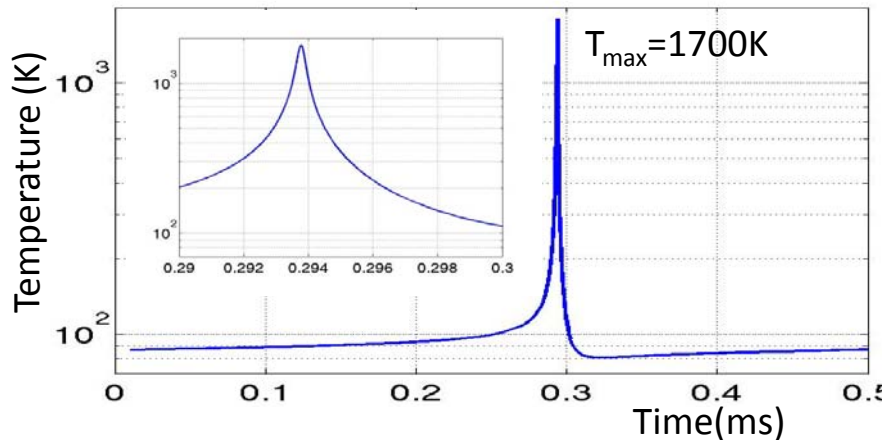
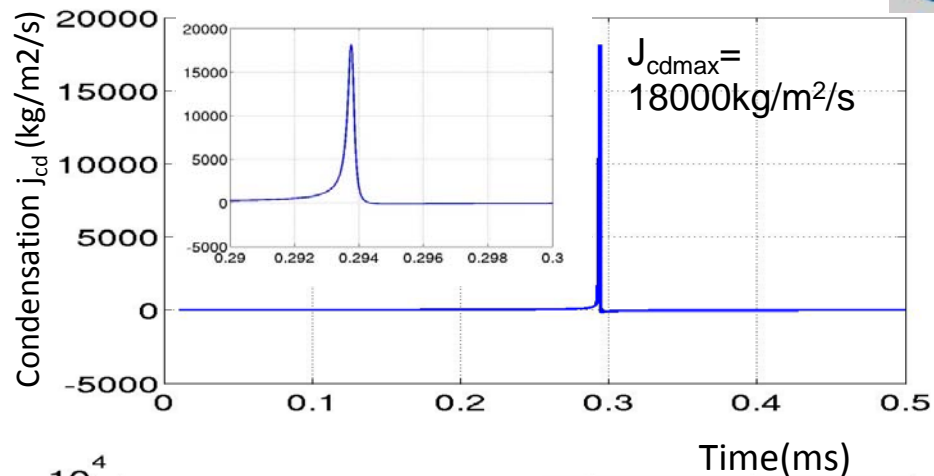
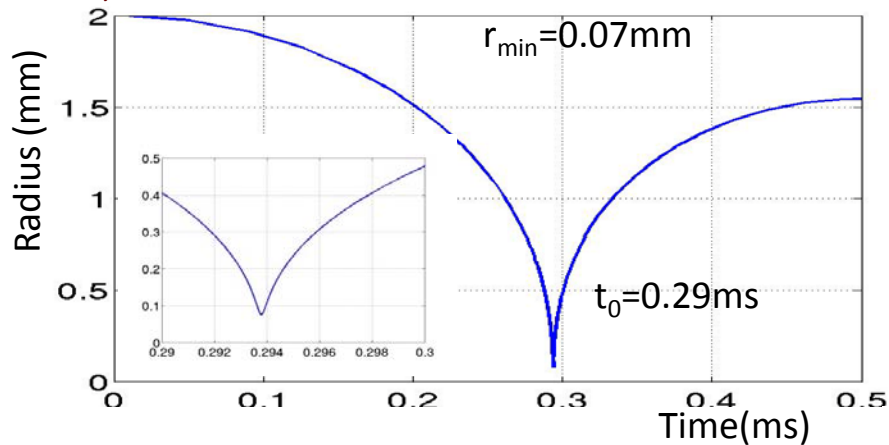
Pressures of the shock waves induced by impact of the LOx fragment at solid surface

$$p \approx \rho_L v^2 / 2 \approx 2.5 \text{ atm}, v = 20 \div 30 \frac{m}{sec}$$

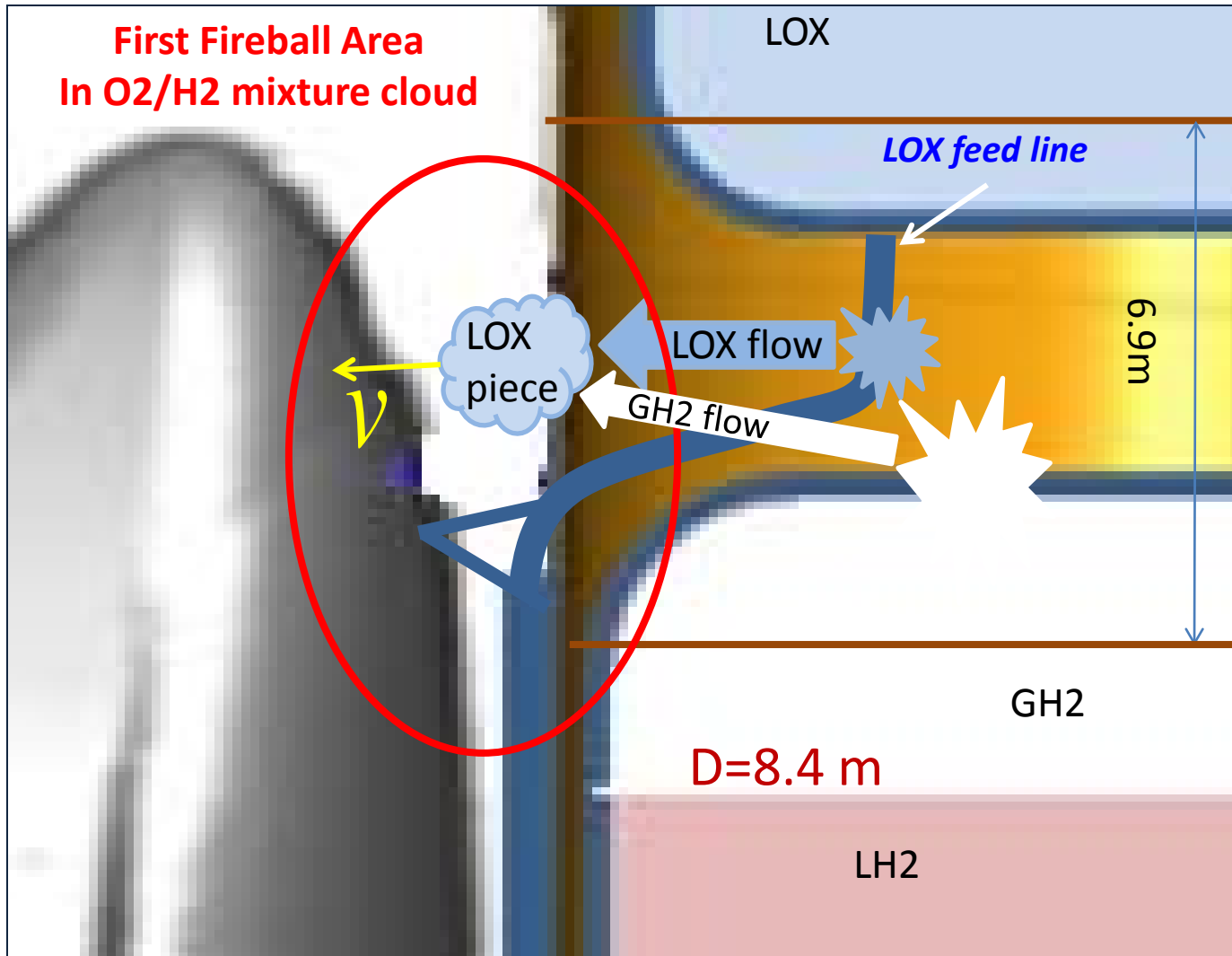
Collapsing of bubble of radius $r_0=2\text{mm}$, temperature $T_L=90\text{K}$, pressure $p=1\text{atm}$, and initial partial GH2 pressure 0.003atm (red), 0.01atm (blue) under the initiating shock wave with over pressure $\Delta p_L=0.5\text{atm}$ (red), 1atm (blue). (see next slide for detail).

Conclusion: The pressure in the weak shock wave is too small to directly induce ignition of GH2/GOx mixture of any composition but is large enough to induce bubble collapse in the liquid oxygen.

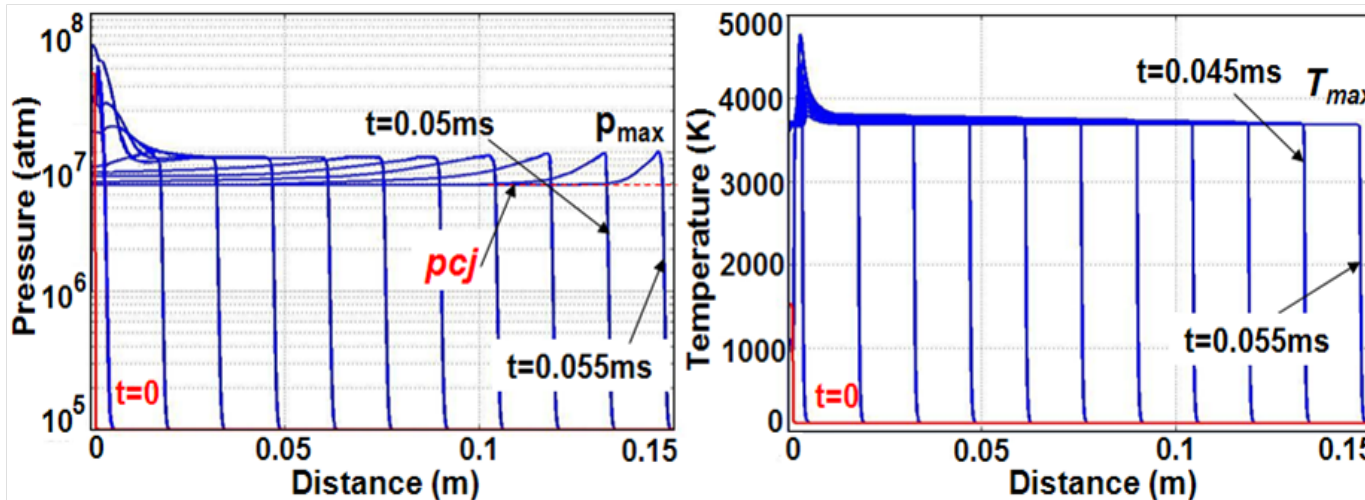
Nov. 5-8, 2012



Shock formation in LOx pieces as a result of their impact on Challenger surface and cavitation-induced ignition of released GH2/Ox (Scenario 2)



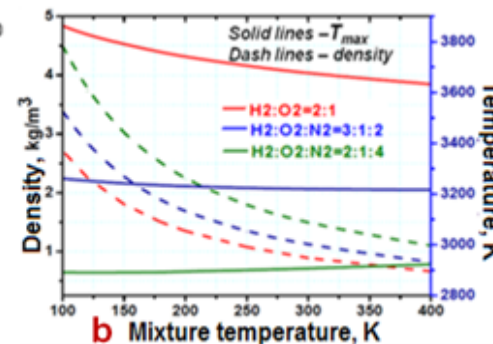
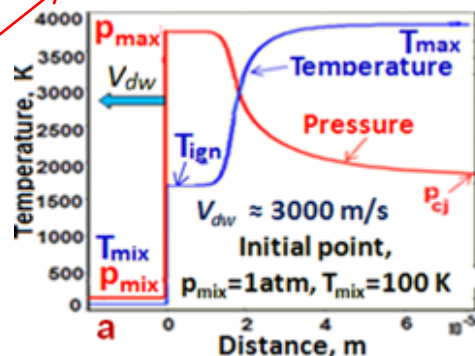
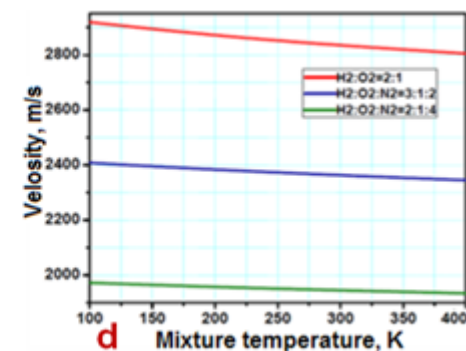
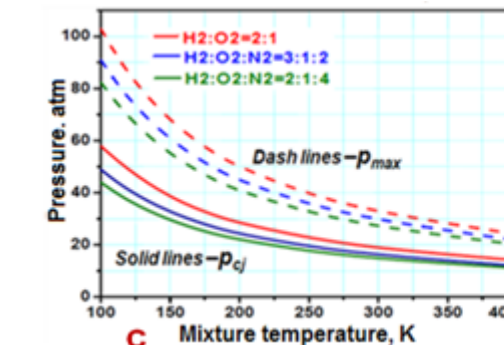
Dynamics of detonation wave formation in gaseous stoichiometric H₂/O₂/N₂ mixture induced by cavitation ignition



Numerical and analytical calculations showed that the pressure in the collapsing bubbles can exceed 2000 atm. Radial shock wave of the radius $r > 0.15\text{mm}$ and the pressure $p > 250\text{atm}$ induced by a collapsing bubble can lead to detonation ignition of the H₂/O_x mixture. Dynamics of this process is shown in the figures.

Cavitation-induced ignition of a stoichiometric H₂/O_x mixture (2:1) with the mixture temperature $T=100\text{K}$ and pressure $p=1\text{atm}$ for radius $r > 0.15\text{mm}$. Initial cavitation condition: temperature $T_0=1500\text{K}$ and pressure $p_0=350\text{atm}$ for $r < 0.15\text{mm}$ (in red).

The parameters of steady detonation wave $p_{\text{max}}=100\text{atm}$, $p_{\text{cj}}=60\text{atm}$, $T_{\text{max}}=3800\text{K}$, $v_{\text{dw}}=3000\text{m/s}$ in stoichiometric H₂/O_x mixture coincide with those that we obtained using the model (CANtera) taking into account 19 main chain reactions in GO_x/GH₂ mixture detonation.



Ignition induced by injection of hot atom gases from bubbles collapsing in a liquid into GH₂/GO_x mixture



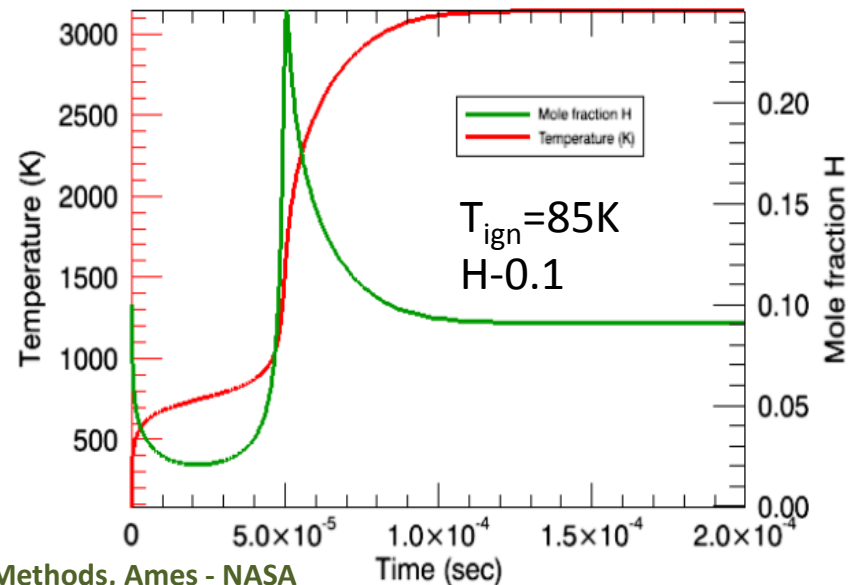
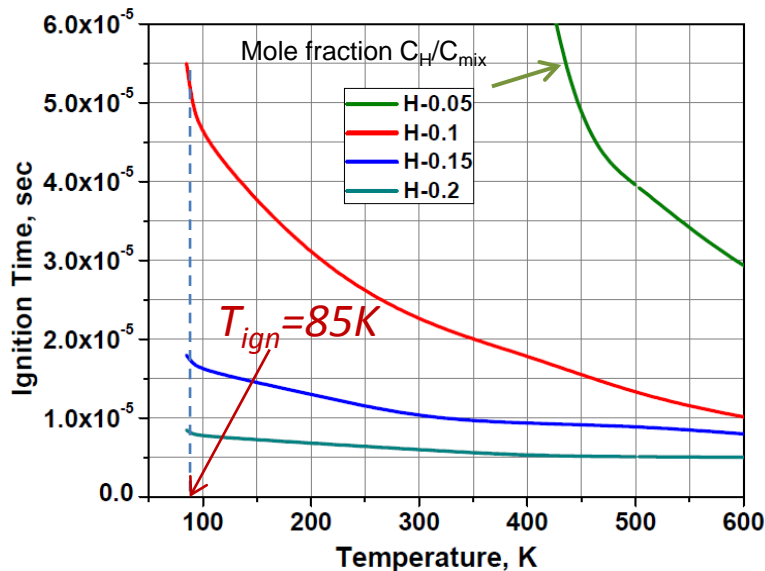
In reality the super-hot and compressed O, H, and OH species are formed in the process of GH₂/GO_x combustion inside bubbles. They will be ejected into the space above the LO_x surface and easily ignite the GH₂/GO_x mixture nearby

In the case of injection of the atomic species into the explosive H₂/O_x mixture the ignition rates is limited by the following very fast reactions:



The first and last reactions have activation energy $\Delta=0$ and other Δ is closed to zero.

Our calculation based on CANTERA Code showed that the explosive mixture containing 0.05 mole fraction of atomic hydrogen self-ignites at the temperatures $T \geq 85K$.

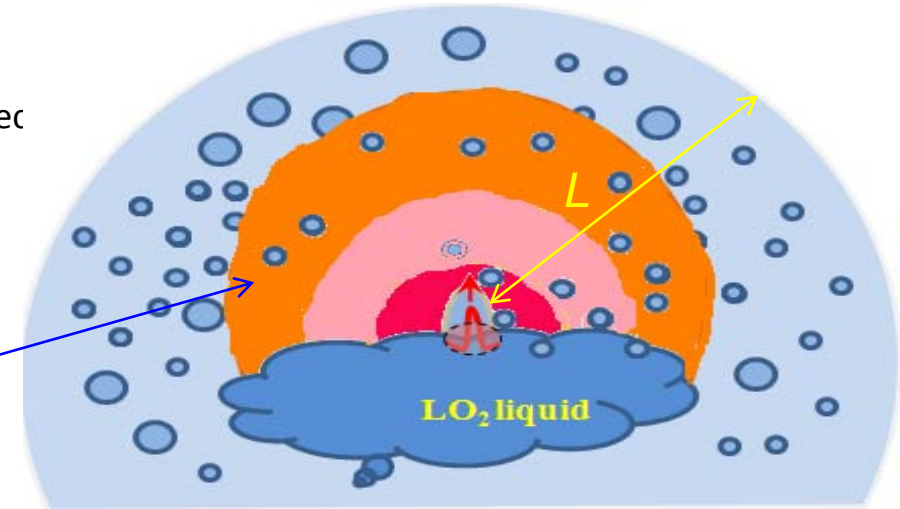
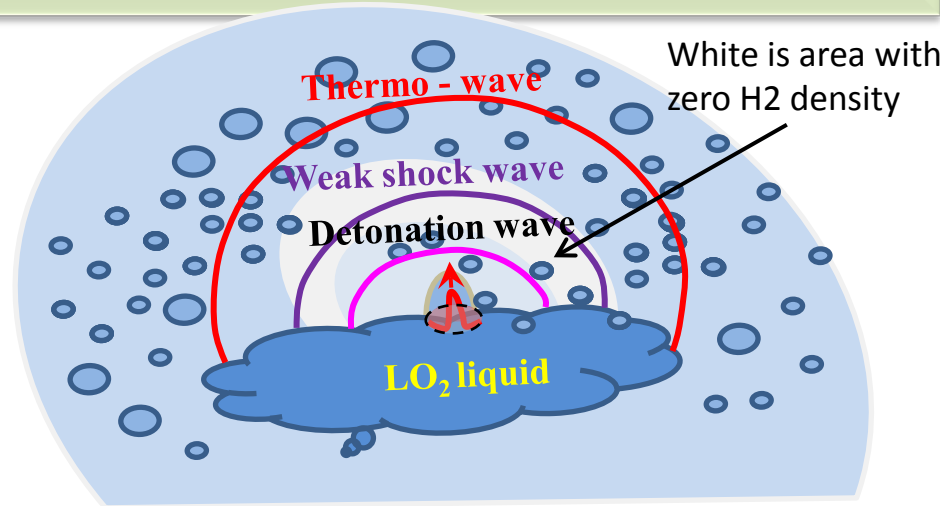
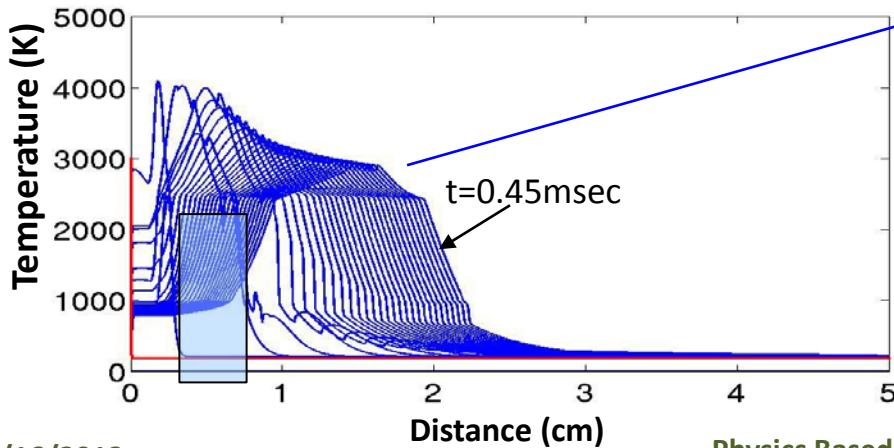
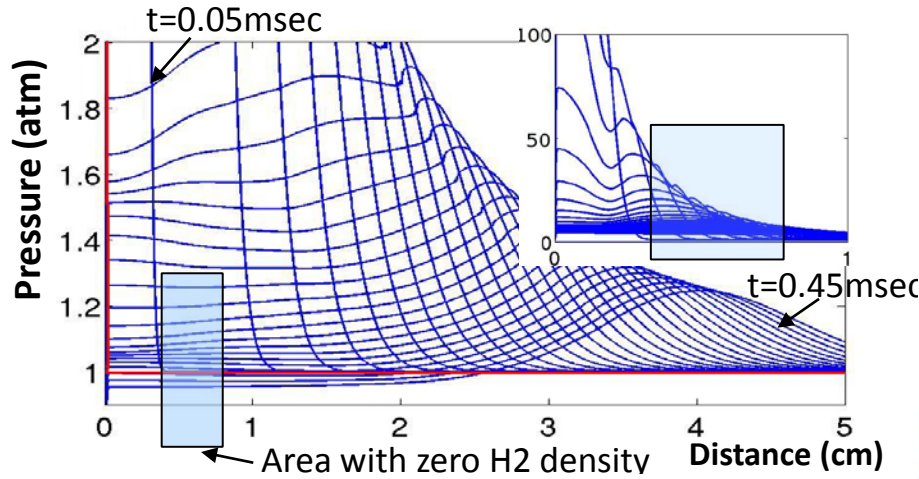
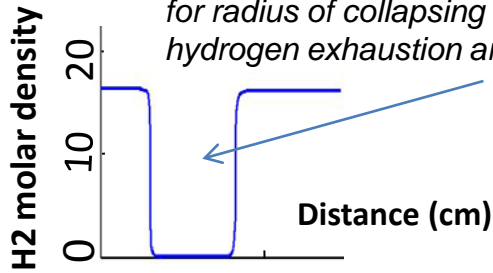


Transition of local detonation induced by cavitation ignition to aerosol deflagration)

Results of simulation

for radius of collapsing bubble $r_{min}=0.1mm$, size of hydrogen exhaustion area $R_{inh}=1cm$

Initial conditions:
 $T_{mix}=200K$, $p_{mix}=1atm$;
 $T=3000K$, $p=3000atm$
inside area $r < r_0=0.1mm$;



The detonation wave rapidly dissipates in the area with zero H2 density and heat wave initiates a deflagration in the mixture at the other side of zero H2 area.

The parameters of the deflagration wave:

Maximum temperature $T_{max}=2600K$,

Flame front velocity $V_f=30m/s$, Pressure p is about 1atm

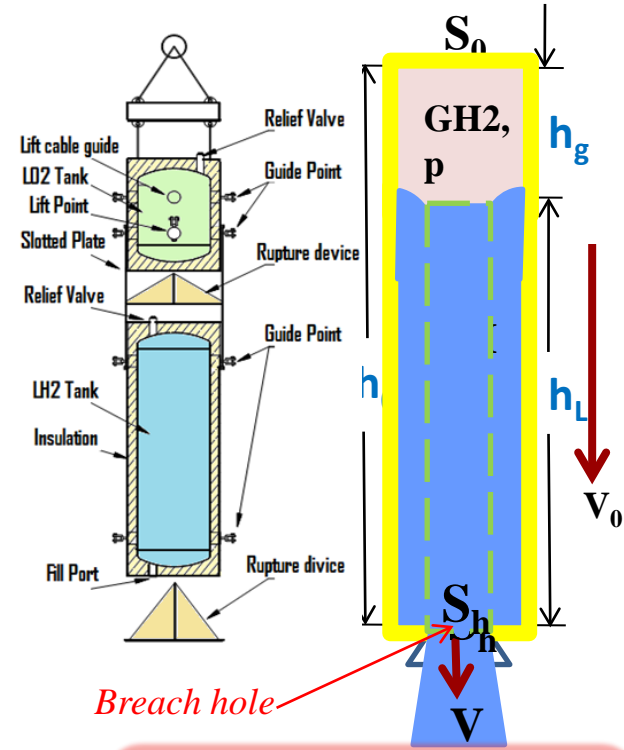
Proposed mechanism of the explosion of GH2/GOX mixture

- HOVI test explosions of GH2/GOX mixture are intensified by the combustion of cryogenic H₂/O₂ aerosols
- Aerosol vaporization is controlled by infrared radiation of hot combustion products
- Aerosols form as a result of an impact of the liquid jet escaping from the ruptured tanks against solid surfaces.

Sequence of events leading to explosion

1. Breach of the LH2 tank and escape of the LH2 jet
2. Fragmentation of the LH2 jet and formation of LH2 droplets (aerosol) in the air
3. Partial evaporation of LH2 droplets
4. Breach of the LOx tank and formation of LOx aerosol cloud near the top of the LH2 tank
5. Mixing of LH2 and LOx aerosols
6. Cavitation-induced ignition upon direct contact of large LOx pieces with LH2 droplets
7. Onset of **fast deflagration** combustion of LH2 with atmosphere oxygen and formation of hot luminous combustion products
8. Enhanced LH2 and LOx droplet evaporation by infrared radiation
9. Initiation of radiation-mediated LH2-LOx aerosol combustion behind the flame front
10. Rapid flame acceleration as a result of pressure, temperature, and product density buildup due to the aerosol combustion
11. Formation of a **super-fast deflagration or detonation** flame that may trigger deflagration-to-detonation transition
12. Formation of detonation due to cavitation-induced ignition

Dynamics of escape of H₂ and Ox liquids from ruptured tanks (the first group of HOVI Tests)



Breach hole

$$V_{\max} = V_{g0} \left(\frac{p_{at}}{p_0} - \frac{\rho_L v_0^2}{2p_0} \right)^{-1/2}$$

Maximum volume of escaped LH₂ occur in tanks with relatively large initial gas volume V_{g0} or when bottom (but not tops) of tanks are ruptured (group 2 HOVI)

Conservation of mass of escaped liquid in time dt (adiabatic process)

$$\frac{\rho_L v^2}{2} S_h dh = \frac{\rho_L v_0^2}{2} S_h dh + (p - p_{at}) S_h dh, \quad dh_g = -dh_L = \frac{S_h}{S_0} v dt, \quad dm_L = \rho_L S_0 dh_g,$$

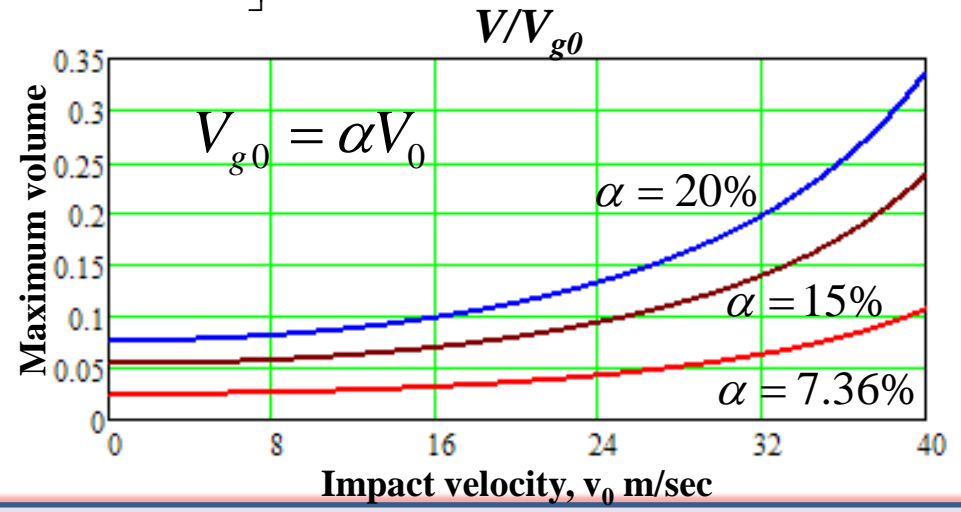
$$\frac{p}{p_0} = \left(\frac{V_{g0}}{V_g} \right)^\gamma \quad \frac{dV_g}{dt} = a \left(\left(\frac{V_{g0}}{V_g} \right)^\gamma - \frac{p_{at}}{p_0} + \frac{\rho_L v_0^2}{2p_0} \right)^{1/2}, \quad a = \frac{S_h}{S_0} \left(\frac{2p_0}{\rho_L} \right)^{1/2}$$

$$t = \int_{V_{g0}}^{V_g} \frac{dV}{a \left[\left(\frac{V_{g0}}{V} \right)^\gamma - \frac{p_{at}}{p_0} + \frac{\rho_L v_0^2}{2p_0} \right]^{1/2}}$$

$$\frac{\rho_L v_0^2}{2p_0} < \frac{p_{at}}{p_0}$$

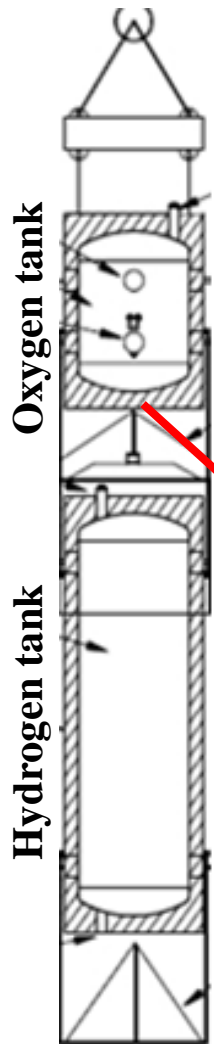
Hydrogen is a light liquid

for impact velocity $v_0 < 45 \text{ m/sec}$



Maximum volume of escaped LH₂ does not depend on the ignition delay time and hole cross-section S_h

$$\rho_L = 70 \text{ kg/m}^3, \quad \gamma = C_p/C_v = 1.4, \quad p_0 = 1.45 \text{ atm}, \quad p_{at} = 1 \text{ atm}$$



$$t = \int_{V_{g0}}^{V_g} \frac{dV}{a \left[\left(\frac{V_{g0}}{V} \right)^\gamma - \frac{p_{at}}{p_0} + \frac{\rho_L v_0^2}{2p_0} \right]^{1/2}}, \quad a = S_h \left(\frac{2p_0}{\rho_L} \right)^{1/2}$$

$$V_g(t) \approx V_{g0} + t S_h \left(\frac{2p_0}{\rho_L} \right)^{1/2} \left(\frac{\rho_L v_0^2}{2p_0} - \frac{p_{at}}{p_0} + \left(\frac{h_{g0}}{h_0} \right)^\gamma \right)^{1/2}$$

for $t \leq t_{esc} = h_{ot} / v_0 \approx 25m \text{ sec}$

LOX flow t_{ex} is time of escape of the main column of Ox liquid of cross section S_h

Maximum volume of escaped liquid

$$\eta_m = \frac{S_h}{S_0} + \frac{h_m - h_g(t_{ex})}{h_0 - h_g(t_{ex})} \approx 33\%$$

for the delay time about 180m sec

Maximum volume of escaped Ox liquid can occur only when bottoms (but not tops) of both tanks are ruptured (group 1) and there is a relatively large delay time

$V_0=33m/s$ – velocity of the tank on impact; V_{g0} and p_0 are initial volume and pressure of gas in the O_2 tank

$$\rho_L = 1141kg / m^3, \quad \gamma = C_p / C_v = 1.4$$

$$p_0 = 2.1atm, \quad p_{at} = 1atm$$

$$\frac{\rho_L v_0^2}{2p_0} > \frac{p_{at}}{p_0}$$

Oxygen is a heavy liquid

for impact velocity $v_0 > 13m / \text{sec}$

$$V_m = V_{g0}(t_{ex}) \left(\frac{p_{at}}{p_1} \right)^{-1/2} \quad \text{for } t > t_{esc}$$

The time of the fall of the escaped Ox liquid to the ground

$$t_{ex} = (h_{H2} + h_{O2}) / v \approx 100m \text{ sec}$$

$h_{H2} = 2.24m$ and $h_{O2} = 0.86m$ are heights of hydrogen and oxygen tanks

Breach of H_2 tank top results in escape of gaseous H_2

Dynamics of escape of gaseous H_2

V_{g0} and $p(0)$ are initial volume and pressure of gas in the H_2 tank,
 S_h – cross section of the rupture

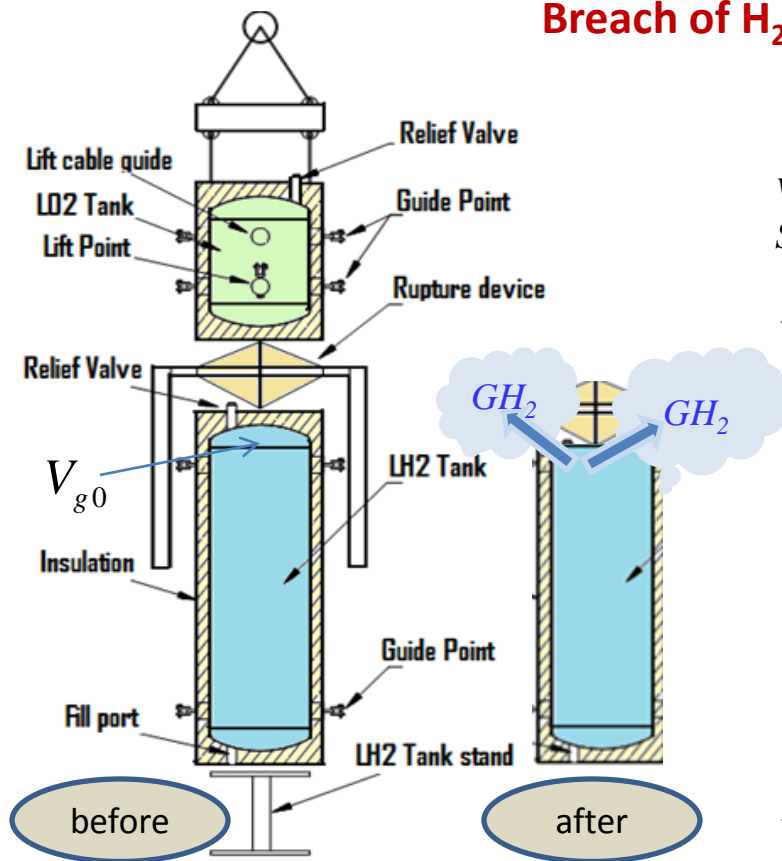
$$V_{g0} \frac{d\rho_v}{dt} = -jS_h, \quad S_h = \pi r_h^2,$$

$$p = R_v \rho_v T,$$

$$j(t) = \left(\frac{p_0}{p} \right)^{1/\gamma} \sqrt{\frac{2\gamma}{\gamma-1} p \rho_v \left(1 - \left(\frac{p_0}{p} \right)^{1-1/\gamma} \right)}$$

$$M_{H_2} = S_h \int_0^{t_{esc}} j dt, \quad M_{H_2}^{max} \approx \frac{p(0) - p_0}{p_0} \rho_v V_{g0}$$

*Time of escape t_{esc} is determined by the area S_h
Total escaped mass M_{H_2} does not depend on S_h
For $r_h > 10\text{cm}$ escape time t_{esc} is less than
the explosion delay time τ_d*

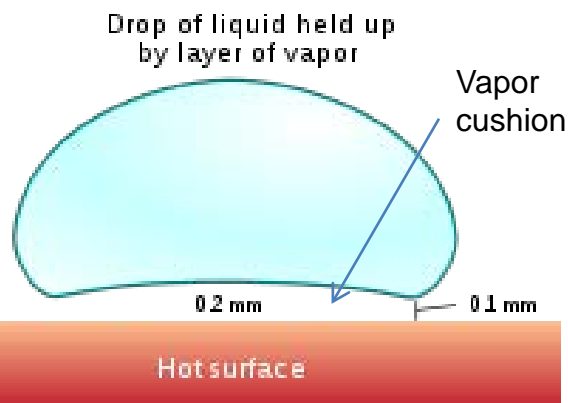


For $r_h > 10\text{cm}$

$M_{H_2} = 0.9\text{kg}$ for HOVI 5 and

$M_{H_2} = 0.5\text{kg}$ for HOVI 2.

Evaporation is slowed down by film boiling



A vapor cushion forms between the liquid and hot solid surface (**Leidenfrost effect**). Due to this effect a drop of water that is vaporized almost immediately at 334 °F (168 °C) persists for 152 seconds at 395 °F (202 °C).

We emphasize that in the case of LH2 spills the temperature of the ground is 15 times higher than the boiling temperature of the liquid.

The equation for the height of vapor cushion:

$$\frac{q_h \rho_L \rho_v g}{12 \mu \kappa_v (T_0 - T_L)} \frac{d}{dr} \left[r h^3 \frac{d}{dr} \left(h + a^2 \frac{d^2 h}{dr^2} \right) \right] = \frac{r}{h}$$

Characteristic length scales of:
vapor cushion **thickness** and droplet **radius**

$$h_0 \propto \left(\frac{\mu_v \kappa_v (T_0 - T_L) a^2}{q_h \rho_v \rho_L g} \right)^{1/5} \quad a = \sqrt{\frac{\sigma_L}{\rho_L g}}$$

Estimating evaporation time t_0 :

$$\pi R^2 q_h \rho_L H \propto \pi R^2 t_{L, \text{evap}} \kappa_v (T_0 - T_L) / h_0$$

$$t_{L, \text{evap}} \propto \frac{q_h \rho_L H h_0}{\kappa_v (T_0 - T_L)}$$

For $R = H = 5\text{mm}$ $t_0 = 5\text{sec}$

Predicted evaporation time is very **long** in comparison with conductivity time $t_{\text{evap}} = 30\text{msec}$.

Vapor pressure must balance the hydrostatic pressure:

$$p(r) = p_{\text{atm}} + (H - h(r)) \cdot \rho_L g - \sigma_L \frac{\partial^2 h}{\partial r^2}$$

p_{atm} – the atmospheric pressure, h – the cushion height as a function of radius, H – max drop height

$$q(r) \propto \frac{\kappa_v (T_0 - T_L)}{h(r)} \quad \text{-steady conductive heat flux}$$

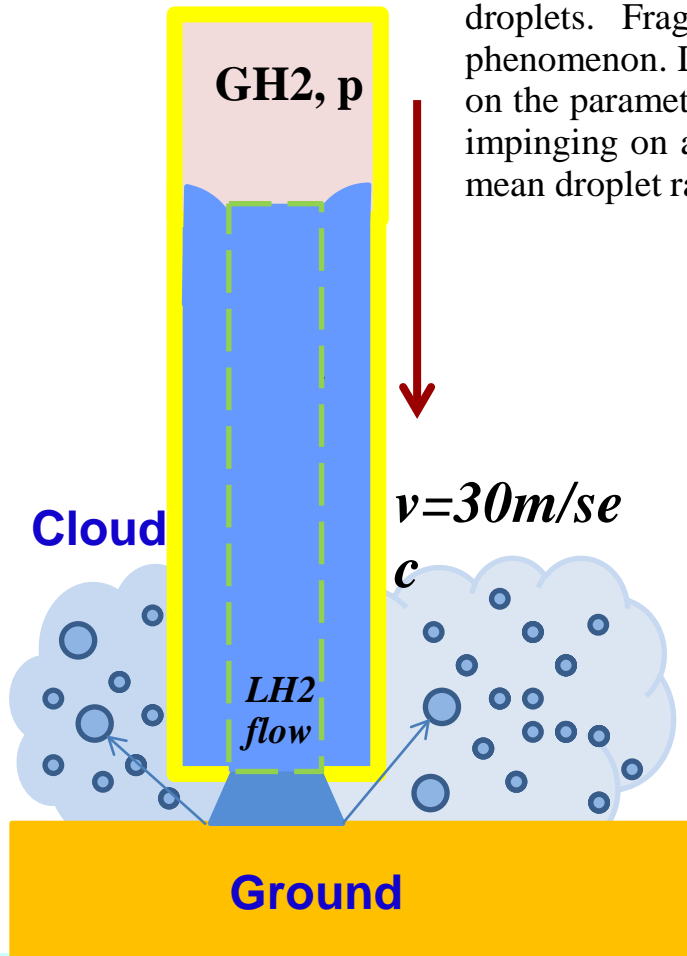
Conservation of vapor mass:

$$\bar{v}(r) \propto \frac{\int_0^r r' q(r') dr'}{q_h \rho_v r h(r)} \quad \text{-average radial vapor velocity balancing evaporation flux}$$

Stokes equation, lubrication approximation

$$\frac{dp}{dr} \propto -\frac{12 \mu \bar{v}(r)}{h^2(r)} \quad \text{-Darcy's law}$$

Fragmentation of escaped liquids and formation of droplets



Impact of the liquid jet with the ground results in turbulence and breaks the liquid into droplets. Fragmentation of liquid droplets is a complex and poorly understood phenomenon. Droplet sizes may vary significantly. The typical droplet radius depends both on the parameters of the liquid and gas [1]. Very recent experimental studies of liquid jets impinging on a flat smooth surface established the following empirical correlation for the mean droplet radius [2]:

$$r_d = 2.53 \times 10^5 d_{or} \text{Re}^{-1.28} \text{We}^{0.4} \left(\mu_{\text{LH}_2} / \mu_{\text{air}} \right)^{-1.16},$$

$$\text{Re} = \frac{d_{or} v \rho_L}{\mu_{\text{LH}_2}} - \text{Reynolds number}, \quad \text{We} = \frac{d_{or} v^2 \rho_L}{\sigma_{\text{LH}_2}} - \text{Weber number},$$

dynamic viscosity of air $\mu_{\text{air}} = 1.63 \times 10^{-5} \text{ Pa sec}$,

and hydrogen $\mu_{\text{LH}_2} = 1.32 \times 10^{-5} \text{ Pa sec}$, $\mu_{\text{LO}_2} = 1.96 \times 10^{-4} \text{ Pa sec}$

Typical droplet radius

$$r_{d,\text{H}_2} \square 8\text{mm}, \quad r_{d,\text{O}_2} \square 0.5\text{mm}$$

Typical radius of the droplets in the H₂ cloud is about r_{d,H₂}=8mm and in the O₂ cloud is about r_{d,O₂}=0.3mm. These values are almost independent of the stream diameter d_{or}.

[1] Lei Xu, Wendy W. Zhang, and Sidney R. Nagel, "Drop Splashing on a Dry Smooth Surface", PRL 94, 184505 (2005).

[2] M. Ahmed, N. Ashgriz and H. N. Tran, "Influence of Breakup Regimes on the Droplet Size Produced by Splash-Plate Nozzles", AIAA JOURNAL Vol. 47, No. 3, 516-522 (2009).

μ - viscosity
 v - flow velocity of liquid,
 ρ_L - 70 kg/m³ - density
 d_{or} - stream diameter
 σ - surface tension

11/16/2012

Radiation-induced evaporation-burning of a hydrogen droplet

Two mechanisms of the heat transfer from the hot gas (combustion products) to cold H2 droplet:

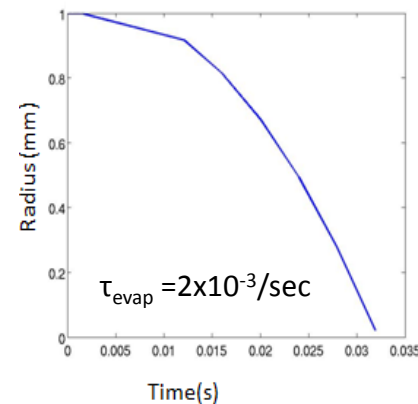
- (i) thermo-conduction and (ii) infrared radiation of hot gas.
- (i) The thermo-conduction evaporation is surface heating of a droplet to a temperature T_s due to diffusion heat flow of hot gas.
- (ii) Radiation heat is volume process ($\alpha_{abs} r_{bubble} < 1$) that results in heating of whole droplet to T_L and fast evaporation and burning.

Equations describing evaporation and burning LH2 droplet are the same that used for bubble cavitation with the exception of the equation for radius

$$\rho_L \dot{R} = \rho_g (u_g - \dot{R}) = j_{cd},$$

$$j_{cd} = \frac{\beta (p_{Ox} - p_s(T_s))}{\sqrt{2\pi R_{Ox} T_s}},$$

$$p_s(T_s) = p_c \left(\frac{T_s}{T_c} \right)^\lambda$$



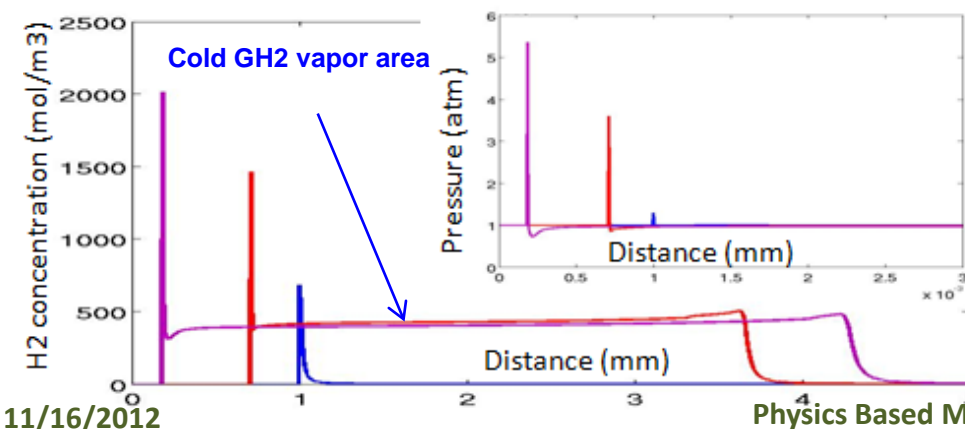
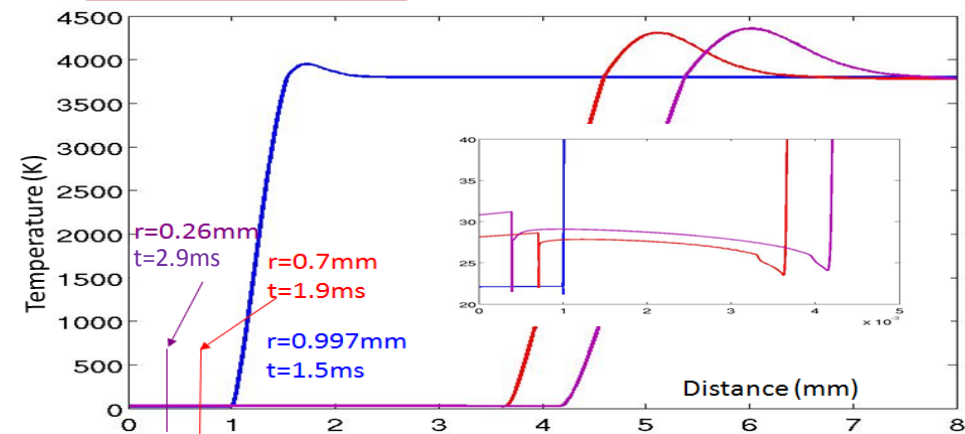
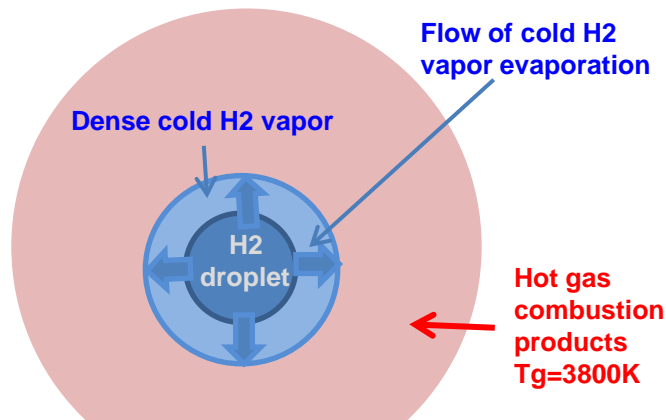
The conduction flow is depressed due to cold GH2 vapor area near the droplet. Therefore the evaporation time a bubble with $R_0 > 1\text{mm}$ can be estimated ($T_c = 33.2\text{K}$ is critical temperature)

$$(T_c - T_{L0}) C_L \rho_L V_R = (\alpha R) \varepsilon \sigma T_g^4 S_R t, \quad t_{evap} = \frac{C_L \rho_L (T_c - T_{L0})}{3\alpha \varepsilon \sigma T_g^4}$$

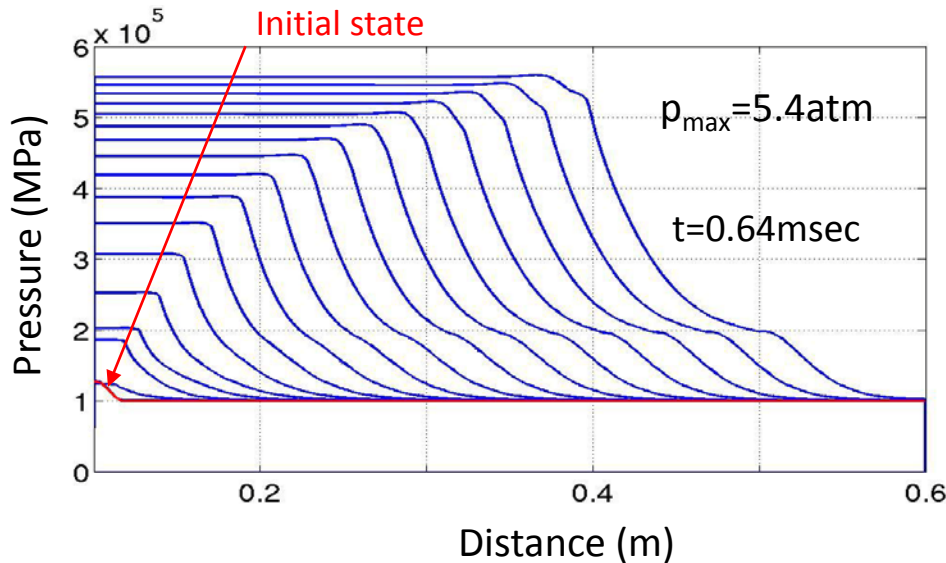
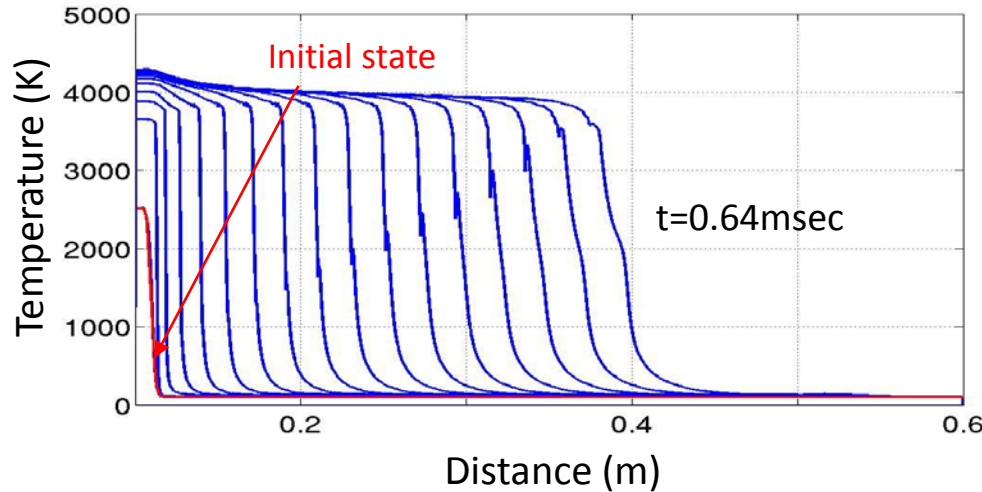
Radiation-induced combustion

$$d(\rho H_2)/dt = -(\rho H_2/\tau_{evap})(T(t)/T_0)^4$$

$$T_0 = 3500\text{K}, \quad \tau_{evap} = t_{evap}/e = 10^{-3}/\text{sec.}$$



The super-hot and compressed O, H, OH species are formed in the collapsed bubble in process of a local explosion the GO_x/GH₂ mixture inside the collapsing bubble. These species can be ejected from the bubble into the space above the LO_x interface and easily ignite the GH₂/GO_x mixture localized under this interface. This effect can induce the fast deflagration of the aerosol mixtures.



The time of radiation-induced combustion

$$\tau_{evap} \approx \frac{1}{e} t_{evap} \approx \frac{C_L \rho_L (T_c - T_{L0})}{10 \alpha \epsilon \sigma T_g^4}$$

does not depend on the droplet radius and averaged density of droplets can be presented as

$$d(\rho_{H2drop})/dt = - \rho_{H2drop} / \tau_{evap} (T(t)/T_0)^4$$

$$T_0 = 3500K, \tau_{evap} = 10^{-3}/sec.$$

The value of $\rho_{H2drop} / \tau_{evap}$ was added in the mass balance equations for the gas components. The results are depended on relation of the averaged droplet density to the evaporation time: $\rho_{H2drop} / \tau_{evap}$.

Initial averaged droplet density
 $\rho_{H2drop}(0) = 0.05 kg/m^3$ $r = 6 \div 8$ mm
 $\rho_{O2}(0) = 0.4 kg/m^3$ $r = 0.5$ mm

Parameters of flame front

Velocity $V_f = 620$ m/sec, Temperature

$T_{max} = 3900$ K, Pressure $p_{max} = 5.5$ atm

HOVI test	Pressure sensor data, atm	Experimental shock velocity*	Calculated shock velocity	Mass and density of H ₂ aerosol, M _{H2} kg, (ρ _{H2} =kg/m ³ , M _{O2}	Duration of shock (calculated and measured)
13	3.3÷4.2	≈ 740÷825	≈ 760	≈ 0.7kg (0.031kg/m ³) 5.6 (0.248)	≈3.5msec
5	2.5÷3	≈ 660	≈ 660	≈ 0.45kg (0.02) 3.6 (0.16)	≈4.0msec
2	3.2÷5.4	≈ 780	≈ 785	≈ 0.65 kg (0.029) 5.2 kg (0.23)	≈3.4msec
9	80÷110	2625÷2966	2500÷2928	8.3÷15.2kg (0.68) 66-121kg (5.44)	≈0.7msec

- ❑ The HOVI test data showed that a liquid hydrogen spill alone is not likely to self-ignite, because in every HOVI test with a ground cloud of hydrogen, caused by a breach in the bottom of the hydrogen tank, the ground cloud did not ignite until liquid oxygen was released. The ignition occurs when gaseous hydrogen (GH₂) and oxygen (GO_x), and liquid oxygen (LO_x) mixture is available.
- ❑ LO_x stream released from the tank serves to ignite the GH₂/GO_x mixture via the collapse (cavitation) of vapor bubbles in LO_x. The ignition effect intensifies when GH₂ is contained in the bubbles. Such bubbles can form from the turbulent mixing of H₂ and O_x flows escaping from the breached fuel tanks. Very high pressures and temperatures arise in the collapsing bubbles due to ignition of the GH₂/GO_x mixture inside the bubbles.
- ❑ Super-compressed and hot gases injected from a bubble near LO_x surface into GH₂/GO_x mixture produces a strong shock wave, followed by hot gas. This cavitation-induced ignition can lead to deflagration or detonation of GH₂/GO_x mixtures. The combustion characteristics depend on volume, structure and composition of the H₂ and O_x clouds.
- ❑ Impact of the liquid jet with the ground results in turbulence and breaks the liquid into droplets that are partially evaporated and form aerosol clouds with gaseous H₂ and O_x present. The aerosol combustion determines the main parameters of the explosion including high pressure, temperature and flame front velocity. Its rate is controlled by the infrared radiation of hot combustion products.
- ❑ The aerosol combustion can result in detonation of GH₂/GO_x mixture when H₂ and O_x gases and aerosols are well-mixed. Our calculation show that such a situation is realized in the HOVI 9 test and determines the high explosion yield in this case.
- ❑ In the case of poorly mixed H₂ and O_x clouds the aerosol combustion cannot result in detonation but intensifies deflagration, i.e., it increases the pressure, temperature and flame front velocity (HOVI 13 and 14 tests of the first group).
- ❑ In the second group of the HOVI tests (HOVI 2 and 5) only GH₂ has time to escape form the top of the tank before the explosion, i.e. the LH₂ aerosols do not arise. Therefore, deflagration occurs with relatively low pressure, temperature and flame front velocity.